DOKUZ EYLÜL UNIVERSITY
GRADUATE SCHOOL OF NATURAL AND APPLIED SCIENCES

NUMERICAL SIMULATION OF PHASE CHANGE WITH NATURAL CONVECTION INSIDE AN ANNULAR SPACE

by
Arife Elif GENÇER

September, 2019
İZMİR

NUMERICAL SIMULATION OF PHASE CHANGE WITH NATURAL CONVECTION INSIDE AN ANNULAR SPACE

A Thesis Submitted to the
Graduate School of Natural and Applied Sciences of Dokuz Eylül University
In Partial Fulfillment of the Requirements for the Degree of Master of Science
in Mechanical Engineering, Thermodynamics Program

by
Arife Elif GENÇER

September, 2019
İZMİR

M.Sc THESIS EXAMINATION RESULT FORM

We have read the thesis entitled **"NUMERICAL SIMULATION OF PHASE CHANGE WITH NATURAL CONVECTION INSIDE AN ANNULAR SPACE"** completed by **ARİFE ELİF GENÇER** under supervision of **ASSOC. PROF. DR. MEHMET AKİF EZAN** and we certify that in our opinion it is fully adequate, in scope and in quality, as a thesis for the degree of Master of Science.

Assoc. Prof. Dr. Mehmet Akif EZAN

Supervisor

Prof. Dr. Aytunç EREK

(Jury Member)

Asst. Prof. Dr. Mustafa ASKER

(Jury Member)

Prof. Dr. Kadriye ERTEKİN

Director

Graduate School of Natural Applied Sciences

ACKNOWLEDGEMENTS

I would like to thank my supervisor, Assoc. Prof. Dr. Mehmet Akif EZAN, for all his help, to conduct this research and his willing to teach which I always admire. This study would not have been possible without his valuable assistance. I also thank Prof. Dr. Aytunç EREK for his valuable contributions.

Foremost, I would like to thank my parents Nihal and İskender GENÇER, and also my brother, Gökçe Mehmet GENÇER, and additionally to my sister, Funda GENÇER, for their endless support for this study. I always feel privileged to have such a family that whenever I need help, they support me. I wish to express my gratitude to them because of their patience.

Finally, I would like to thank all my friends who are not only from university or childhood friend but also at Lisi Aerospace. I always feel their endless support. Especially, I would like to thank my friend Fazıl Erinç YAVUZ, because of his all helps and endless support from initial to end of the study.

Arife Elif GENÇER

NUMERICAL SIMULATION OF PHASE CHANGE WITH NATURAL CONVECTION INSIDE AN ANNULAR SPACE

ABSTRACT

Natural convection has an important role in the thermal processes, thermal energy storage systems, and phase change problems. Because of this reason, natural convection is an important aspect to be focused and needed to be taken into consideration for efficient system design.

The objectives of this thesis the investigation of the natural convection occurred in the cylindrical annulus and the effects of the natural convection on the phase change problem. Within this context, two main problems are investigated. First one is the natural convection inside a cylindrical annulus. A 2D model is established in MATLAB® to observe the natural convection phenomenon for air and water domains. Governing equations are reduced into algebraic sets of equations by using finite volume method. In conclusion, when Prandlt number is at seven for water and temperature differences increases, Nusselt number increases up to four centigrade degrees, then decreses up to approximately nine centigrade degrees then increase again for different ratio of differences of inner and outer radii to inner radii. Numerical results are validated, making use of the available experimental data from the literature. Secondly, phase change inside the cylindrical annulus is investigated for various parameters, i.e., outer wall temperature, the initial temperature of the ice and aspect ratio of the cylindrical annulus. When inner wall temperature is at four, eight and fourteen centigrade degrees for aspect ratio is at two, four and eight, melting times are compared. Then, this observations are done for same temperatures and aspect ratios for outer wall. These numerical results as well are compared with the literature findings a satisfactory agreement is found between the numerical results and experimental literature data.

Keywords: Heat transfer, natural convection, cylindrical annulus, mathematical model, phase change

HALKASAL BOŞLUKTAKİ DOĞAL TAŞINIMLI FAZ DEĞİŞİMİNİN SAYISAL SİMULASYONU

ÖZ

Doğal taşınım termal işlemlerde, ısıl enerji depolama sistemlerinde ve faz değişim problemlerinde önemli role sahiptir. Bu sebepten dolayı, doğal taşınım, verimli sistemlerin dizaynlarında odaklanılan ve hesaba katılması gereken önemli bir bakış açısıdır.

Bu tezin hedefi silindiriksel boşlukta oluşan doğal taşınımı ve doğal taşınımın faz değişimine etkisini araştırmaktır. Bu bağlamda, iki temel problem araştırılmıştır. Birincisi, silindiriksel boşluktaki doğal taşınımdır. Su ve hava alanlarında, doğal taşınımı gözlemlemek için MATLAB® da 2D model kurulmuştur. Korunum denklemleri sonlu hacimler yöntemi ile cebirsel denklem kümelerine indirgenmiştir. Sonuç olarak, Prandlt sayısı su için yedi iken sıcaklık farkı arttığında, farklı iç-dış silindir yarı çap farkının iç yarı çapa oranları için, Nusselt sayısı dört santigrad dereceye kadar artmış, sonra yaklaşık dokuz dereceye kadar azalmış, sonra tekrar artmıştır. Sayısal sonuçlar, literatürdeki uygun deneysel veriler kullanılarak doğrulanmıştır. Ikinci olarak silindiriksel boşluktaki faz değişimi, dış duvar sıcaklığı, buzun başlangıç sıcaklığı, silindiriksel boşluğun oranı vb. çeşitli parametreler için araştırılmıştır. Farklı iç dış silindir çapı oranları için, iç duvar sıcaklığı dört, sekiz ve on dört santigrad derece olduğunda, erime süreleri karşılaştırılmıştır. Sonra, bu gözlemler aynı sıcaklık ve aynı iç dış silindir çapı oranları için dış duvarda yapılmıştır. Bu sayısal sonuçlar, literatür bulguları ile kıyaslandığında, sayısal sonuçlar ile deneysel literatür verileri arasında tatmin edici bir uzlaşmaya varıldı.

Anahtar sözcükler : Isı transferi, doğal taşınım, silindiriksel boşluk, matematiksel model, faz değişimi

CONTENTS

LIST OF FIGURES

LIST OF TABLES

Page

CHAPTER ONE
INTRODUCTION

The natural convection heat transfer is the transfer of heat without any external force, and it is a mechanism which is encountered in various thermal design problems. In other words, natural convection is an essential phenomenon since it plays an active role in lots of thermal applications such as cooling of electronic devices, nuclear reactors, and designing of solar energy collectors. Different type of fluids, both liquids, and gases are examined in this topic, and movement of fluids is observed as the fluid density changes with temperature.

Convection is a type of heat transfer mechanism which occurs between a surface and fluid because of the temperature difference which is between them. Convection has two types. One of them is forced convection, and the other one is natural convection. In forced convection, fluid moves with external influence like fans. However, in natural convection, movement of fluids occurs by itself because of the difference of temperature, which is in the fluid. Major bases of natural convection are the movement desire of fluid that is heated. Heated fluid wants rises because its density decreases. Another word, when the fluids are heated, the density of fluids goes down and vice versa when the fluids are cooled, fluid density increases. However, some fluids, such as beryllium or water, have an important characteristic that is called density inversion. Density inversion is the difference of density variations, which is up to a specific temperature that is special to fluid and after that temperature. For this topic, water is one of the best examples. Because, while water's density increases up to 4°C, after this temperature, it starts to decrease. In other words, 4°C is the density inversion point of water.

There are numerous studies, both numerical and experimental, that deal with the steady or transient natural convection in cartesian, cylindrical or spherical coordinates. The current thesis considers the natural convective heat transfer inside a cylindrical annulus with and without phase change. That is, the literature review section is focused on the works that are related to the natural convection inside cylindrical annulus only.

1.1 Literature Review

Kuehn and Goldstein (1976) investigated local velocity, temperature, and heat transfer coefficients of natural convection in horizontal cylindrical annulus numerically and experimentally. Mach-Zehnder interferometer is used in order to determine the temperature variations and experimental local heat transfer coefficients. Rayleigh number was changed from 2.11E+4 to 9.76E+5, and they used the finite difference method in order to solve the equations.

Seki, Fukusako, & Nakaoka (1975) conducted one of the most extensive experimental studies in the literature about natural convection heat transfer. They studied about effect of the density inversion of water between horizontal concentric cylinders on natural convection heat transfer. Seki et al. (1975) experimented the effect of density inversion of water on the natural convection between two concentric horizontal cylinders. Diameters of cylinders changed between 1.18 and 6.39. Water has a maximum density at 4°C. While the temperature of the inner wall is 0°C, the outer wall temperature is changed from 1 to 15°C. At the same time, the Grashof number was changed from 3.2E+1 to 2.7E+5. As a result of this study, the effect of density inversion and average Nusselt number which is a function of temperature differences between inner and outer radii, have in an unexpected way quietly large conversely non-density inversion fluids.

Heat energy is the sum of the kinetic and potential energy of the atoms and molecules which creates material. It occurs the results of atomic or molecular vibrations. Heat energy is stored as perceptible heat, latent heat, reaction heat, or a total of these according to changing of internal energy of the material.

Materials take heat from ambient or give heat to ambient during the phase change. This heat is named latent heat. Phase change materials (PCMs) need to have large latent heat storage ability. After the heat stored, they should be able to give back the heat reversibly without degradation. The required volume to store the latent heat is smaller than sensible heat storage systems volume. For this reason, Thermal energy storage systems (TESs) are considerably popular in last few years.

PCMs are materials which store the latent heat energy as thermal heat energy. In other words, PCMs are special materials that store a large amount of heat like energy during the phase change at a constant temperature. These materials have an ability to absorb and release the energy in a cyclic manner with the reversible solid-liquid phase-change processes.

Although PCM is used in various applications, the calculation procedure for the phase change problems relying on the natural convection could be costly since. Constructed mathematical models require a smaller time step and high mesh intensities. Instead of solving flow and energy equations together, one can consider the effects of convection by defining the effective thermal conductivity. In this way, the problem can be reduced to a conduction problem with phase change. Although there are various Nusselt correlations which are known that effective thermal conductivity for air which depends on Rayleigh number and Nusselt number, there are no correlations for PCM. At the same time, water is one of the most appropriate PCM for cold storage units. Environmental problems have increased with new technological improvements recently. At the same time, energy cost increases and energy sources decrease. So, TESs are more preferable because of being usable and low-cost.

Using of PCMs has got popularity because of their high latent heat ability. Using of PCM is the best technique of TES. This issue has been studied for recent years. TES is used in order to be able to balance when the supplied energy and demanded energy is mismatched. PCMs are used for a lot of industrial application such as; cooling of electrical devices, solar energy systems, buildings, and photovoltaic panels.

Heat exchangers have a significant role in various engineering systems such as; heat recovery unit and process industries. Designing of a heat exchanger is an important issue to build up a feasible system both considering the economical and energetically point of views (Bhutta et al., 2012). For this reason, Computational Fluid Dynamics (CFD) approach is a favorite and preferred method. CFD approach is used for solving the physical problems by means of computational analyses. CFD approach includes, fundamental balance equations, i.e., governing equations, are resolved numerically. The governing equations are first transformed into algebraic equations for discrete elements, i.e., control volumes, and then resolved iteratively to evaluate the velocity, pressure and temperature distributions within the whole system with a lower cost and in a shorter time (Bhutta et al., 2012). However, varying all design and working alternatives in an experimental utility is quite expensive and a time-consuming process. That is, the CFD is used for various design problems of heat exchangers such as; design and optimization of the fluid flow paths, reduction of the pressure drop within the system and improvement of the rate heat transfer with using various types of inserts such as fins or buffers (Bhutta et al., 2012).

Medrano et al. (2009) experimentally investigated solidification and melting periods of five different heat exchanger designs, which are considered as a candidate for a latent heat storage system. They used commercial paraffin RT35 as PCM at the one side of the heat exchanger, and the other side of the heat exchanger is filled with water. They compared each heat exchanger design by considering the average thermal power values. Results show that average power per unit is much more with a double pipe heat exchanger which are located in graphite matrix (approximately between 700–800 W/m^2-K) In other respects, the compact heat exchanger has the largest average thermal power due to extend heat transfer area. Dolado, Lazaro, Marin & Zalba (2011) analyzed the heat transfer difference between the performance of TES models which is improved in order to simulate the heat exchanger which perform with air-PCM and air and PCM which is supplied commercially and capsuled plate macro. Models are based on a formulation which was dimensional conductivity analyses and thermophysical data that are measured in the laboratory by used finite differences method. They used two basic methods in order to be able to carry out the modeling; thermal analyses of a plate and thermal behavior of all the TES unit. Enthalpy and thermal conductivity are determined as a function of the temperature.

When the PCM is chosen according to the application temperature range, the most significant factors considered (Agyenim, Hewitt, Eames & Smyth, 2010);

- The geometry of the PCM tank
- Thermal and geometrical parameters of the tank

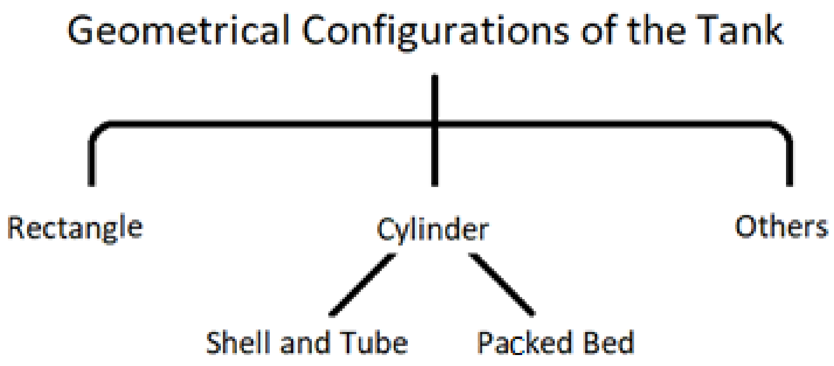

Figure 1.1 Schematic display of the geometrical types of TES tanks (modified from Mao, 2016)

The geometry of TES tanks have an important role on charge and discharge time, heat transfer rate, the temperature distribution of the material in the tank, amount of TES materials, heat exchanger characteristic, i.e., geometries are classified like in Figure 1.1.

Storage tanks have a rectangular and cylindrical shape in general. However, other configurations are still designed and investigated. In Figure 1.2 (a), two basic types of tank configurations are shown. Heat transfer occurs between heat transfer fluid (HTF) and storage materials. Different heat transfer rates are obtained according to different shapes of TES tanks. Configurations of TES tanks are needed to be optimized in order to be able to achieve higher efficiency and lower cost. In the literature, some experiments going on about changing of configurations of TES tanks. Some examples of this are shown in Figure 1.2 (b). Added the more tubes or fins are alternative examples, for other developed configurations (Mao, 2016).

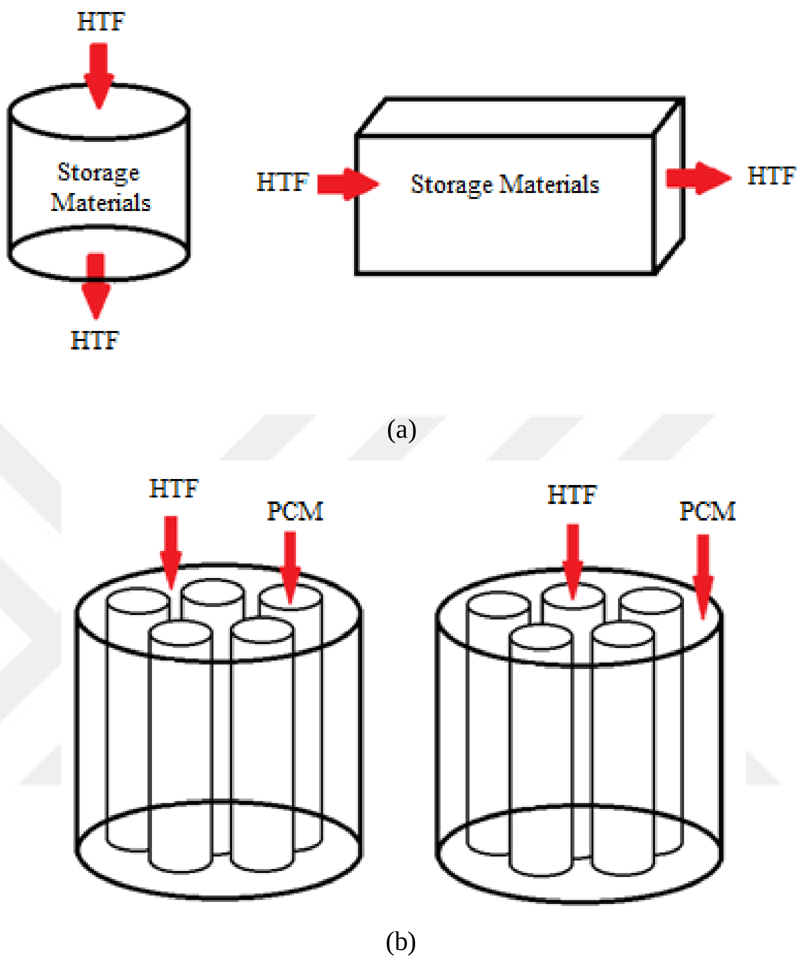

Figure 1.2 Typical TES tank (a) and shell-and-tube cylindrical storage tank (b) (modified from Mao, 2016)

The most common used geometries are rectangular and cylindrical shapes of PCM tanks. Among these, shell-and-tube systems are more investigated than the others due to the lower heat losses (Mao, 2016).

Other examples of PCM systems are given in Figure 1.3. There are mainly three different types of cylindrical PCM containers. In the first type, the PCM is in the shell side, and the HTF flows inside the tube. In the second type, PCM is in the tube, and HTF flows inside the shell. The last cylindrical model involves a shell and a large number of tube system, which increases the heat transfer because of tube numbers (Agyenim et al., 2010).

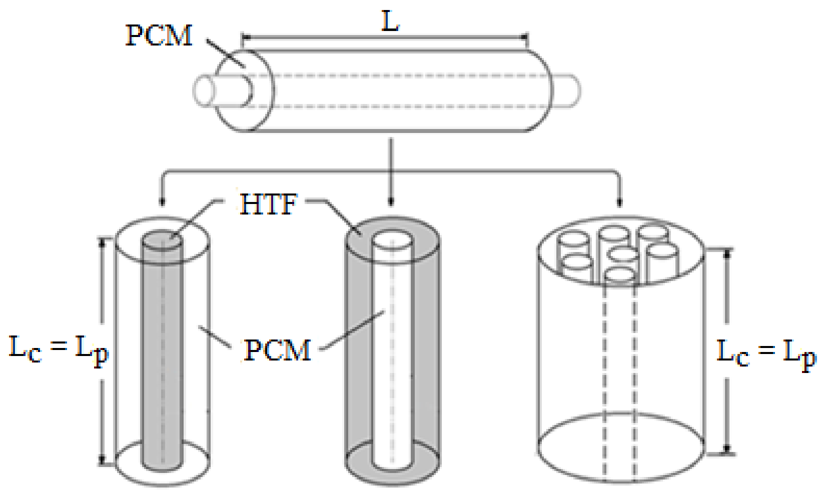

(a) Pipe model (b) Cylinder model (c) Shell-and-tube model

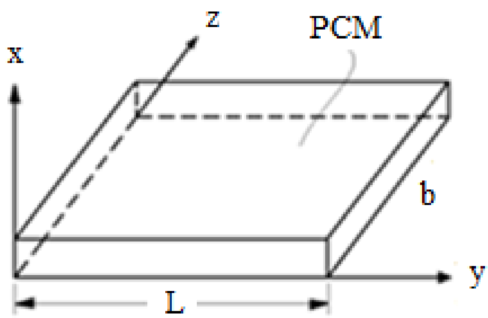

(d) Rectangular or slab container

Figure 1.3 Classification of commonly used shell-and-tube models according to the location of PCM (modified from Agyenim et al., 2010)

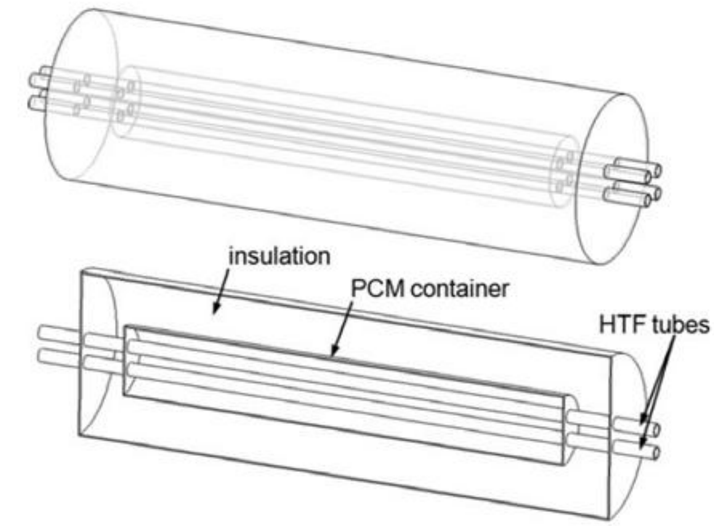

Figure 1.4 Energy storage heat exchanger with multi-tube (Parry et al., 2014)

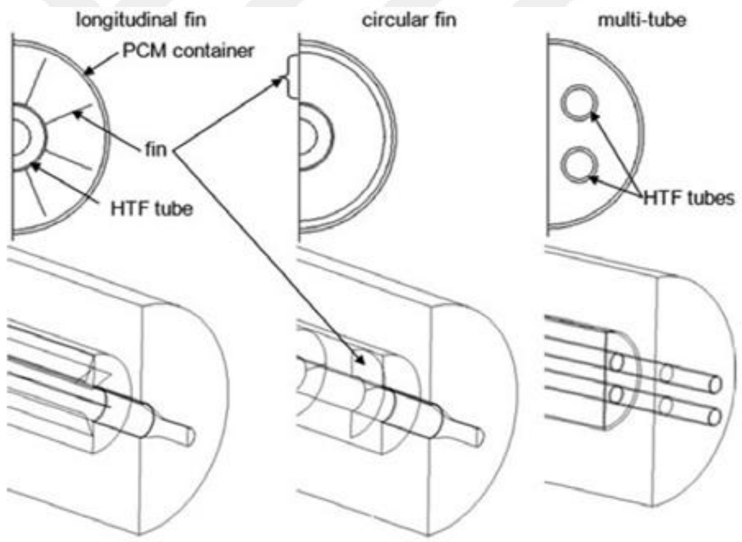

Figure 1.5 Shell-and-tube heat exchangers with different types of fins (Parry et al., 2014)

Parry, Eames & Agynim (2014) studied the improvement of computational simulation of shell-and-tube TES. They investigated and simulated the heat transfer of the systems with a single tube, multiple tubes, single tube with longitudinal and circular fins, and other multiple types. They validate the study with 2D and 3D simulations. Shell-and-tube TES heat exchanger is shown in schematically in Figure 1.4. HTF flows through the tubes where heat transfer occurs, and these tubes are embedded into PCM. There is an insulation layer that covers the PCM tank. Simulated heat exchangers are also tested experimentally. Experimental setups which have different fin types and tube numbers designed as Figure 1.4 and Figure 1.5. When the experiment is realized, all heat exchangers have the same dimensions and are positioned horizontally (Parry et al., 2014).

There are other systems with fin, too. In the last 20 years, a large number of studies are investigated about design and performance of latent heat transfer storage (LHTES) systems in order to be able to increase the heat recovery and observed the effects of design parameters on performance. Fin optimization has two points that need to be considered. First one is costly and the second one is having problems which cause by self-treatment of the system. Two main methods are effective for these studies. One of them is the CFD, and the second one of them is the Lumped Parameters Modelling (LPM). Substantial improvements are progressed about LHTES by means of these two methods. Effects between performance and orientations, length and other similar design parameters of fins are investigated.

Darzi, Jourabian & Farhadi (2016) investigated the solidification and melting of a PCM. They use three different horizontal annulus configurations, which include two circular cylinders. First one is elliptical that is in the circular cylinder. The second one is the circular cylinder with fins. They are investigated numerically in concern with the aspect ratio, positioning of the ellipse, and quantity of fins. They added to copper nanoparticles with various volume fractions into PCM. Thus, they examine the effects of nanoparticles on the rate of heat transfer. As a result, adding the nanoparticles and fins increased the ratio of melting and solidification. A. Abdullateef, Mat, Sophian, J. Abdullateef, & Gitan (2017) designed and tested horizontal triplex tube heat exchanger (TTHX) with fins which are internal longitudinal and contains phase-change material (PCM). The melting point of used PCM is in the range of 78.15–82.15°C. Consequently, through the axial direction, variances are investigated for different flow rate at the average temperature for PCM. At the same time, the effects of added longitudinal and triangular fins are observed. More significant improvements are obtained from triangular fins relatively longitudinal ones. Therefore, triangular fins are thought more effective in melting PCM. A. Abdullateef, Mat, J. Abdullateef, Sopian, & Al-Abidi (2018) investigated at large triplex-tube heat exchanger, PCM and nano PCM with different fin configurations in order to improve the heat transfer. This issue was studied numerically via the FLUENT software. At the final of this study, increasing the conductivity of PCM was observed plainly visible with Alumina. Melting time with different fin configurations were compared with the case of the PCM without nanoparticle. External fins-nano-PCM model embedded in a large TTHX is the most efficient model for accuring the melting of all PCM in a short time. Deng, Nie, Wei, & Ye (2019) proposed a new fin configuration to increase the heat transfer for LHTES. They investigated the local double-fin at various angles and compare the results with uniform double-fin in which the two fins were placed on the top and bottom. As a result of this study, using local double-fin can greatly increase melting than using the uniformly arranged. They noticed that the conductivity of shell has a notable effect on the melting behaviors of local double-fin. Melting time at an optimum angle were determined by changing the fin length. It is observed that at specific fin length and angle when the temperature of heat transfer fluid is increased, melting time decreased. They found that using longer fins can improve the performance of LHTES. Liu, Sun, & Ma (2005) prepared an experimental rig, and they used stearic acid substituted for heat storage material. They investigated the thermal performance of stearic acid and examined its heat transfer characteristics during the melting processes. They compared the influence of heat flux during melting under different heat flux conditions. At the same time, they designed and fixed a new fin configuration in order to be able to increase the thermal reaction of stearic acid. Consequently, it is obviously observed that fins improved the heat transfer of thermal storage unit of the melting process. Fin mechanisms have an improved ability not only heat conductivity but also natural convection. Also, they investigated and analyzed the effect of fin size. They found that these factor effects are increasing thermal conductivity significantly. Mat, Al-Abidi, Sopian, Sulaiman, & Mohammad (2013) investigated three melting methods in order to melt the PCM. These methods are from the inner tube, outer tube, and both tubes. They studied the internal, external, and internal-external fin enhancement techniques. They aim to improve the heat transfer between the PCM and heat transfer fluid. They compared three different situations mentioned above; inner tube heating, outer tube heating, both tube heating. Also, they observed that the effects of the finned and internally finned tube and fin length on the enhancement techniques to melting of PCM. Pizzolato, Sharma, Maute, Sciacovelli, & Verda (2017) conducted experiments on the condensation of the heat transfer problem at the shell-and-tube latent heat storage units via high conducted fins. They solved the phase change material's fluid-dynamic answer each optimization iterations with Navier-Stokes equations which are augmented with a phase-change porosity term. At the final of this study, melting and solidification could be increased significantly natural convection by using well-designed fins with specifically designed features. They made these features in order to optimize for melting fundamentally different from those optimized for solidification. Rahnama & Farhadi (2004) studied about turbulent natural convection between two horizontal concentric cylinders in the presence of radial fins numerically. As a result in this study, the form of streamlines and temperature contours were obtained for a number of radial fins which are attached to the inner cylinder and number of fins change from 2 to 12. They investigated two types of fin configurations for the case of two and four radial fins in order to reveal the effect of fin height and configuration. They found that local Nusselt number variations which are in the inner cylinder, arrangements of fins do not have any significant effect on heat transfer. At the same time, they observed that longer fins have blocking effects on flow and result of this, the heat transfer rate decreases. They observed that the heat transfer rate is decreased in all configurations when there are no fins with the same Rayleigh number. Rayleigh number increases when Nusselt number prediction increases for all-natural convection problems. Tiari, Qiu, & Mahdavi (2015) examined the thermal characteristics of a finned heat pipe and LHTES numerically. Effects of heat pipe space, numbers of fins and length, and the natural convection influence on the thermal response of the TES unit are investigated. According to obtained results, natural convection has an important effect on PCM, during the melting process. They obtained that when the number of heat pipes is increased, the melting rate increases and base wall temperature decreases. In addition to this, as the fin length increases, the temperature difference within the phase change material in the container, which provides more uniform temperature distribution, decreases. Also, the study shows that the number of fins has no significant effect on the system.

1.1. Motivation and the Content of the Thesis

The natural convective heat transfer mechanism is encountered a lot of thermal design problems. For many years, natural convection of different types of fluids in various geometries is investigated numerically and experimentally. Basically, temperature variations in the fluids which are covered by surfaces at different thermal boundary conditions cause density variations. Because of these density variations, natural movement occurs in the fluid. Temperature-dependent change in density changes linearly for air and other lots of fluids. So, Boussinesq approach is used for this type of fluids (Bergman, Lavine, Incropera, & De Witt, 2011). However, temperature-dependent change in density does not change linearly, and it reverses at a special point for some fluids like beryllium and water. For example, the density of water increases between 0°C and 4°C, when the temperature increases. But density reverses and decreases when the temperature is beyond 4°C. This situation is named as density inversion in literature. Natural convection is also very complicated at 4°C, because of the special occasion of water (Gençer, Ezan, Yavuz, Alptekin & Erek, 2017).

Flow lines and Nusselt number variations which were obtained by Seki, Fukusako, Inaba & Sapporo (1978) are given in Figure 1.6 and 1.7. In Figure 1.6, the right side of the vertical-cavity is constantly at T_C = 0°C, and the left side is at different temperatures. For T_H = 4°C, the convection movement of fluid occurs counterclockwise. When the temperature of the left side at T_H = 6°C, two circulation cells are observed in the system. The direction of the circulation which is at the left side is clockwise, but direction of other circulation cell is counter clockwise. 4°C is the line which separates these two cells. When the left side temperature is at T_H = 8°C, two different circulation cells occur both side of the symmetry axis of the cavity (Gençer et al., 2017).

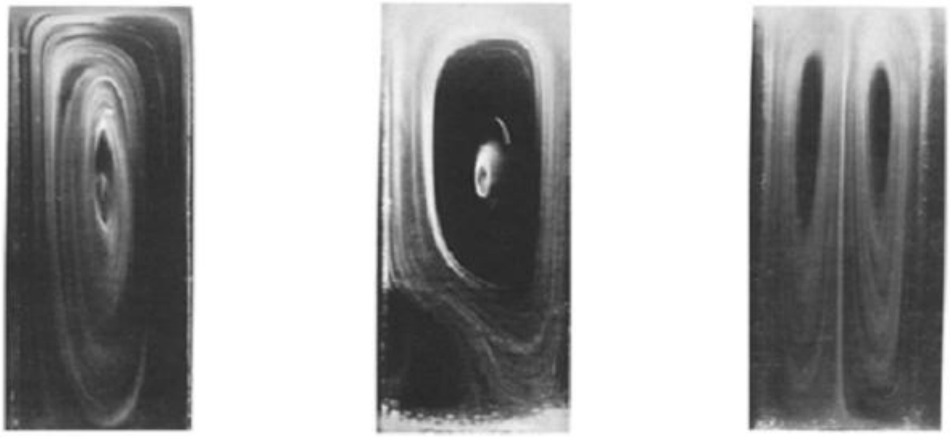

(a) (b) (c)

Figure 1.6 Natural convection of water about 4°C (a) T_C = 0°C, T_H = 4°C, (b) T_C = 0°C, T_H = 6°C, (c) T_C = 0°C, T_H = 8°C (Seki et al.,1978)

The works that are mentioned above are generally examined in cartesian coordinates. There are two main motivations for this study. First one is developing a mathematical model in order to analyze the natural convection of water inside the cylindrical annulus and obtain the variation of Nusselt number near the density inversion temperature. The second one is investigating the phase change of water in the cylindrical annulus. The overview of the thesis content is given below:

- In chapter two, a mathematical model is mentioned for two-dimensional natural convection at the cylindrical annulus. The numerical code is improved in MATLAB®, and the validity of code is compared with the other studies which are in literature for air. The code which is developed in MATLAB® is run for water and compared with the other studies which are in literature.
- In chapter three, the phase change problem with natural convection is investigated. The case of White, Viskanta, & Leidenfrost (1986) is reproduced. The results are compared to the reference work, and time-dependent phase change is observed at determined wall temperature.

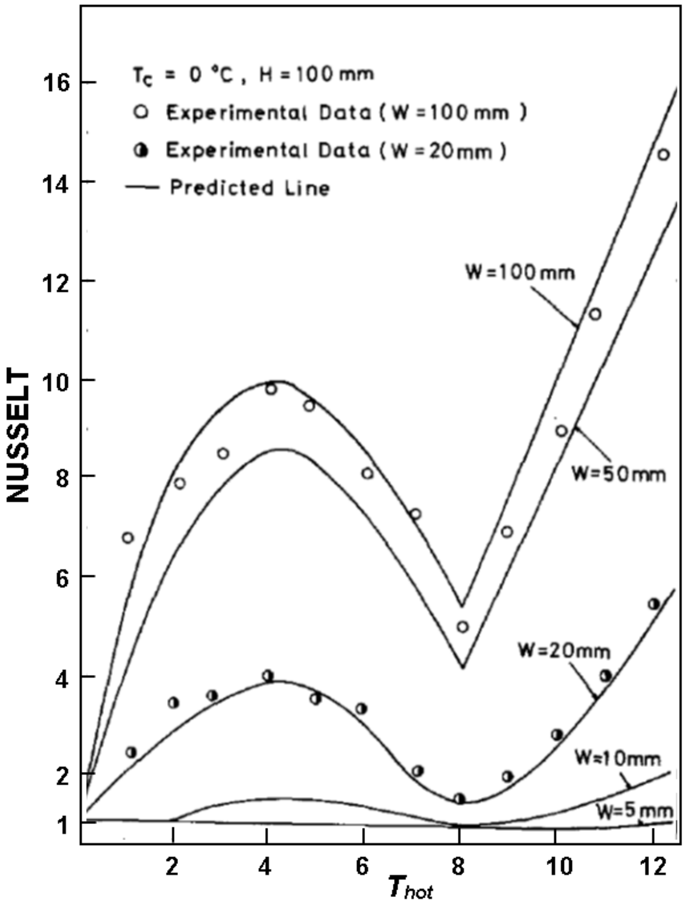

Figure 1.7 Effect of cavity width and temperature differences on Nusselt number (Seki et al.,1978)

CHAPTER TWO
NATURAL CONVECTION INSIDE CYLINDRICAL ANNULUS

In this part of the thesis, natural convection inside a cylindrical annulus is numerically investigated. The model is established in MATLAB® and the Semi implicit method for pressure linked equations (SIMPLE) algorithm is implemented. The numerical model is validated via the analyses made using air as the domain. Previous literature data of Kuehn and Goldstein (1976) is used for the validation process. In order to ensure the validity of code, the current results are compared with experimental data from the literature.

2.1 Definition of Problem

In Figure 2.1, a 2D cylindrical mathematical model is given with boundary conditions. The cylindrical annulus has inner and outer radii of R_{in} and R_{out}, respectively. The other half of the domain is assumed symmetric, and the vertical line is defined as the axis. Inner wall temperature is set as T_{in}, and the outer wall temperature is defined as T_{out}. The calculation domain of the cylindrical annulus is comprised of the air for the validation case. Subsequently, the same domain is established for water in order to analyze the natural convection in the annulus. r-direction is defined from the center of cylinders through the outer surface, and θ-direction is defined from south of the cylinder, i.e., θ = 0°, to north of the cylinder, i.e., θ = 180°. The boundary conditions are defined as follows,

r-direction:

$$r = R_{in} \qquad T = T_{in}, \qquad u_r = 0, \qquad u_\theta = 0 \tag{2.1a}$$

$$r = R_{out} \qquad T = T_{out}, \qquad u_r = 0, \qquad u_\theta = 0 \tag{2.1b}$$

θ-direction:

$$\theta = 0° \qquad -k\left.\frac{\partial T}{\partial \theta}\right|_{\theta=0} = 0, \qquad \left.\frac{\partial u_r}{\partial \theta}\right|_{\theta=0} = 0, \qquad u_\theta = 0 \tag{2.1c}$$

$$\theta = 180° \qquad -k\left.\frac{\partial T}{\partial \theta}\right|_{\theta=\pi} = 0, \qquad \left.\frac{\partial u_r}{\partial \theta}\right|_{\theta=\pi} = 0, \qquad u_\theta = 0 \tag{2.1d}$$

where u_r and u_θ represent the velocity components along with the radial (*r-)* and azimuthal (*θ-)* directions, respectively.

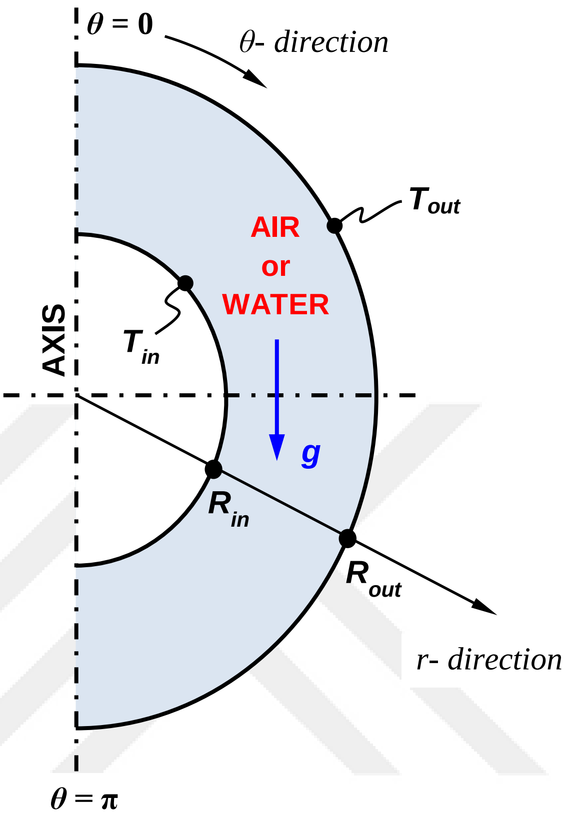

Figure 2.1 2D representation of the calculation domain for the annulus

2.2 Solution Method

For a 2D cylindrical annulus, following conservation equations are considered

Conservation of mass:

$$\frac{1}{r}\frac{\partial (r u_r)}{\partial r} + \frac{1}{r}\frac{\partial u_\theta}{\partial \theta} = 0 \qquad (2.2)$$

Conservation of momentum along r-direction:

$$\frac{\partial u_r}{\partial t} + u_r\frac{\partial u_r}{\partial r} + \frac{u_\theta}{r}\frac{\partial u_r}{\partial \theta} - \frac{{u_\theta}^2}{r}$$
$$= -\frac{1}{\rho}\frac{\partial P}{\partial r} + g_r \tag{2.3}$$
$$+ \vartheta\left[\frac{1}{r}\frac{\partial}{\partial r}\left(r\frac{\partial u_r}{\partial r}\right) - \frac{u_r}{r^2} + \frac{1}{r^2}\frac{\partial^2 u_r}{\partial \theta^2} - \frac{2}{r^2}\frac{\partial u_\theta}{\partial \theta}\right]$$

Conservation of momentum along θ -direction

$$\frac{\partial u_\theta}{\partial t} + u_r\frac{\partial u_\theta}{\partial r} + \frac{u_\theta}{r}\frac{\partial u_\theta}{\partial \theta} + \frac{u_\theta u_r}{r}$$
$$= -\frac{1}{\rho}\frac{1}{r}\frac{\partial P}{\partial \theta} + g_\theta \tag{2.4}$$
$$+ \vartheta\left[\frac{1}{r}\frac{\partial}{\partial r}\left(r\frac{\partial u_\theta}{\partial r}\right) - \frac{u_\theta}{r^2} + \frac{1}{r^2}\frac{\partial^2 u_\theta}{\partial \theta^2} + \frac{2}{r^2}\frac{\partial u_r}{\partial \theta}\right]$$

Conservation of Energy

$$\rho c\left[\frac{\partial T}{\partial t} + u_r\frac{\partial T}{\partial r} + \frac{u_\theta}{r}\frac{\partial T}{\partial \theta}\right] = k\left[\frac{1}{r}\frac{\partial}{\partial r}\left(r\frac{\partial T}{\partial r}\right) + \frac{1}{r^2}\frac{\partial}{\partial \theta}\left(\frac{\partial T}{\partial \theta}\right)\right] \tag{2.5}$$

where g_r and g_ϑ are the components of gravitational acceleration in radial, and polar directions respectively, and ρ is the density of fluid, which is a function of temperature.

Two different approaches are utilized to incorporate the variable density definitions for air and water. Boussinesq approach is used for air to include the buoyancy effect since the density linearly varies as a function of temperature in the case of air. However, in the case of water, the density variation against the temperature has a non-linear behavior, that is, the density is defined as a function of the cell temperature to compute the buoyancy term. For water and air, the following density functions are implemented (Yavuz, 2017),

for air: $\rho(T) = 10^{-5}T^2 - 0.0104T + 3.320$ (T in K) (2.6)

for water: $\rho(T) = -0.007085T^2 + 3.925T + 456.29$ (T in K) (2.7)

The thermophysical properties that are used for air (Pr = 0.7) and water (Pr = 7) are given in Table 2.1.

Table 2.1 Thermophysical Properties (Bergman et al., 2011)

Material	Specific Heat	Density	Thermal Conductivity	Dynamic Viscosity
	(J/kgK)	(kg/m^3)	(W/mK)	(kg/ms)
Air	1005	Eq. (2.6)	0.023	1.6E-5
Water	4180	Eq. (2.7)	0.576	1.0E-3

The SIMPLE algorithm is used to evaluate the transient heat transfer inside the annulus. An iterative solution algorithm is written in MATLAB for the pressure and velocity corrections. The governing equations, i.e., mass, momentum, and energy, are reduced into algebraic sets of equations by using finite volume method of Patankar (1980). Convection terms in the momentum and energy equations are discretized with using Power-Law scheme of Patankar (1980). A uniform mesh structure is preferred in radial and angular directions. The number of the total control volume is defined as 4800 (60×80) according to the preliminary mesh independency analyses.

2.3 Validation of the Study

2.3.1 Natural Convection of Air inside the Annulus

First of all, the model established in MATLAB is for the air domain in order to validate the results with reference to Kuehn and Goldstein (1976).

In Figure 2.2, the variation of Nusselt number depending on Rayleigh number is compared with the literature findings which belong to Kuenh and Goldstein (1976) and Shu, Yao, Yeo, & Zhu (2002). Comparisons show that the current calculated results and the experimental data from the available literature (Kuenh and Goldstein, 1976) are in good agreement. When the Rayleigh number is 100, the Nusselt number is almost unity. The Nusselt number increases as well when the Rayleigh number is increased concerning established. According to this condition, the Prandtl number is 0.7 for air, and the ratio of L/D_{in} is 0.8. L is the annulus gap width and defined as follows;

$$L = R_{out} - R_{in} \tag{2.6}$$

where R_{out} and R_{in} are the inner and outer radii of cylinders, respectively. Rayleigh number is defined as,

$$Ra = \frac{g\beta(T_{max} - T_{min})L^3}{\vartheta\alpha} \tag{2.7}$$

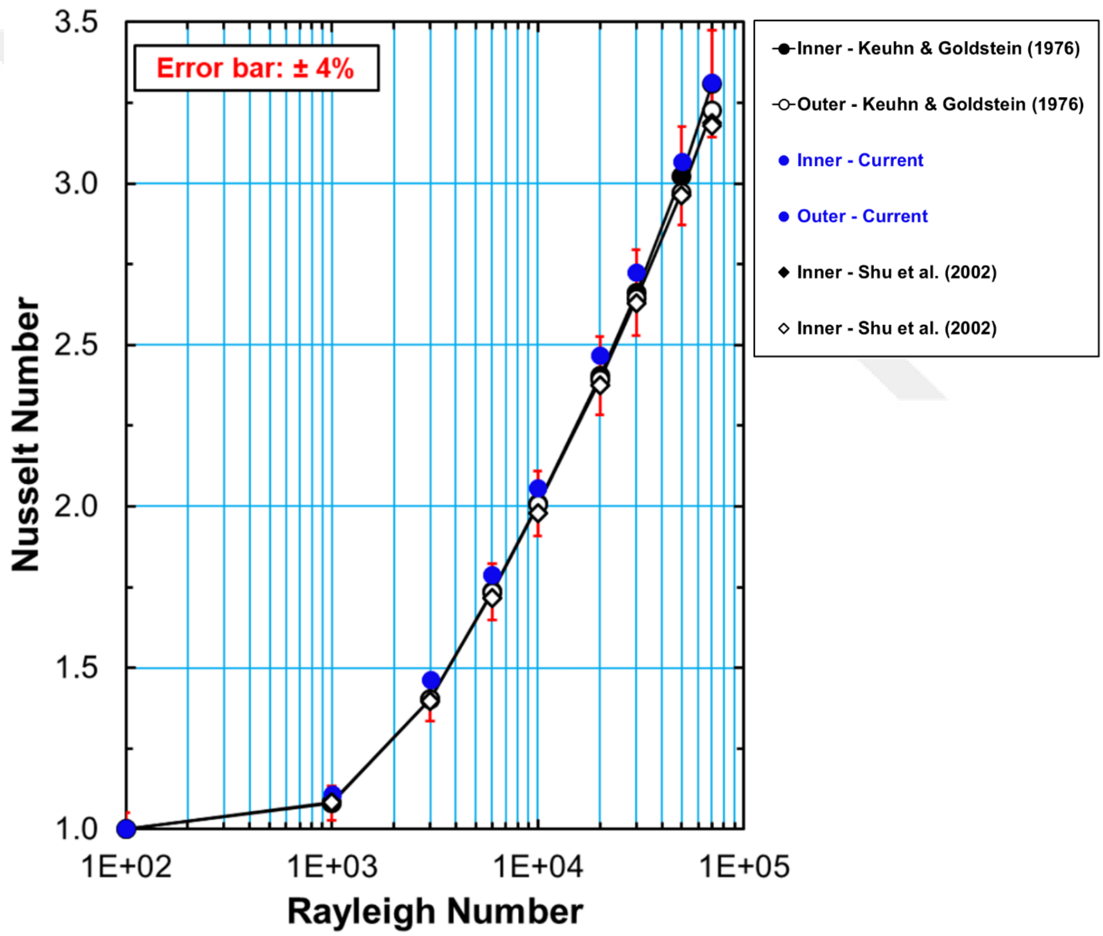

Figure 2.2 Validation of Nusselt number variations (Pr = 0.7, L/D_{in} = 0.8)

In Figure 2.3, the variation of Nusselt numbers on the inner and outer radii are compared with the reference to the same study. Hence, it is observed that the results of the current research and literature yielded in a convincing agreement. In this figure, circle symbols represent the data of the reference study, and straight lines show the results of the current research. In this case, the Prandtl number is 0.7, L/D_{in} is 0.8, and the Rayleigh number is 5E+4. Results which are given in Figure 2.3 obviously show that the variation of Nusselt number increases along the θ-direction from 0° to 180° on the inner cylinder. Besides for the outer cylinder, Nusselt number variation has a different tendency when it is compared to the inner cylinder. Local Nusselt number reduces along the θ-direction from 0° to 180° on the inner cylinder.

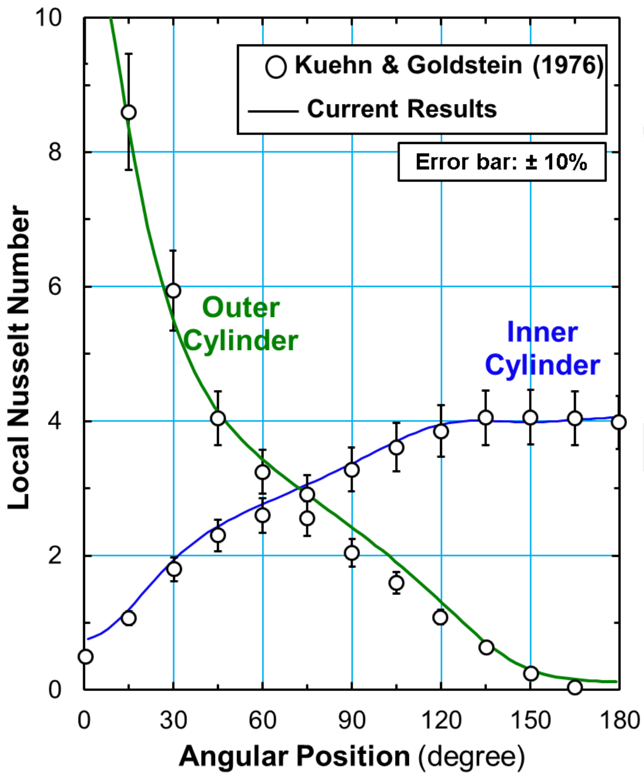

Figure 2.3 Variation of local Nusselt numbers on the inner and outer walls (Pr = 0.7, L/D_{in} = 0.8, Ra = 5E+4)

Temperature distributions and streamlines are shown and compared with the current study and reference article in Figure 2.4. It is observed that the similarity between the calculated results and literature data is satisfactory. When the streamlines are investigated, it can be seen that the center of the annulus gap of the current study is nearly 140° similar to the center of the annulus gap, according to Kuenh and Goldstein. (1976). Moreover, when the temperature distributions are examined, the agreement between the numerical results and literature data is obvious.

Figure 2.4 (b) of the temperature distribution profile; the adjacent lines show that the heat transfer rate is higher in that area. The air next to the inner cylinder gets warmer and moves to the upper side of the annulus; while it gets cold moves to the bottom side of the annulus when it comes near the outer cylinder.

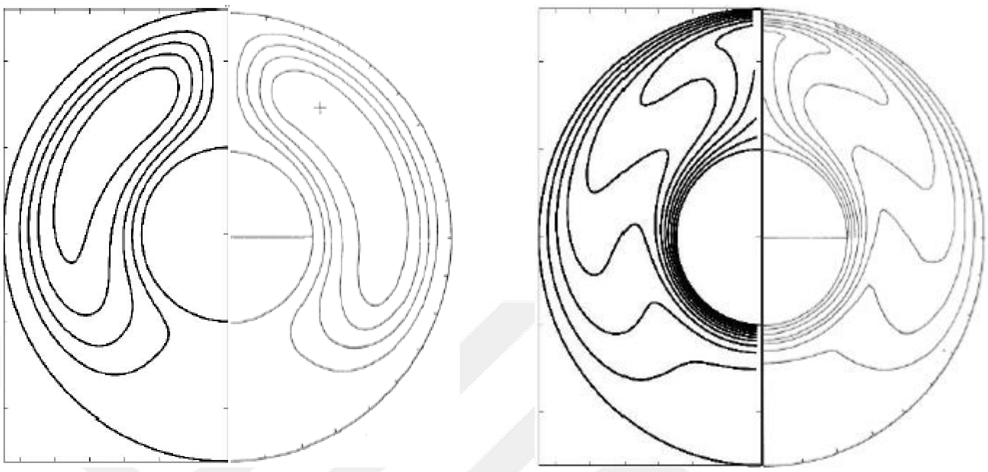

Current Study Kuenh and Goldstein (1976) Current Study Kuenh and Goldstein (1976)

Streamlines (a) Temperature Distribution (b)

Figure 2.4 Comparison of the streamlines and temperature distributions between current study and Kuehn and Goldstein (1976) (Pr = 0.7, L/D_{in} = 0.8, Ra = 5E+4)

2.3.2 Natural Convection of Water inside the Annulus

As the second target, the validated model is used to investigate the natural convection for the water domain in the annulus. Here the results which are obtained from analyses are compared with the references article (Seki et al., 1975). Seki et al., (1975) defined the Nusselt number as,

$$\mathrm{Nu} = \frac{q}{\pi D_{in} \Delta T} \frac{L}{k} \tag{2.8}$$

where q is the rate of heat transfer on the inner cylinder. In order to evaluate a comparative chart with the reference study (Seki et al., 1975), various cases are examined based on the inner case temperature. The temperature of the inner case is increased from 3°C to 10°C with increment steps of 0.5°C. Additionally, these conditions are carried out for various annular gaps (AR = D_{out}/D_{in}). Two different approaches are used in this study. In the first one, Prandtl number is defined as constant, as 7.0; whereas in the second approach, it is defined as a function of the mean water temperature. Nusselt numbers evaluated for the constant Prandtl number approach are given in Table 2.2.

Table 2.2 Nusselt numbers at different annulus aspect ratios and temperature differences

ΔT	Pr = 7			
	AR = D_{out}/D_{in}			
	1.72	3.20	3.44	6.39
	Nusselt Number			
3.0	2.83	10.48	6.87	17.60
3.5	2.83	10.54	6.90	17.61
4.0	2.84	10.51	6.87	17.42
4.5	2.84	10.35	6.76	16.91
5.0	2.69	9.78	6.27	15.29
5.5	2.50	9.27	5.52	12.83
6.0	2.29	8.69	4.78	13.48
6.5	2.13	7.87	4.36	13.48
7.0	2.14	8.00	4.77	14.33
7.5	2.19	8.04	5.69	16.43
8	2.03	9.25	6.55	16.99
8.5	2.32	10.38	7.25	18.69
9	2.61	11.51	7.83	21.50
9.5	2.89	12.36	8.35	22.86
10	3.14	13.22	8.83	24.04

For the second approach, the mathematical model is run again for the same temperature differences and D_{out}/D_{in} ratios. However, as defined previously, the Prandtl number is defined as a function of the temperature. Prandtl numbers are determined according to thermophysical properties of water for each temperature differences. Intermediate Prandtl values are calculated with interpolation. Prandtl numbers are given in Table 2.3 for the selected range.

Table 2.3 Prandtl Numbers at different wall temperatures

ΔT (°C)	**Average Temperature** (°C)	**Pr**
1.00	0.50	13.21
2.00	1.00	12.97
3.00	1.50	12.73
4.00	2.00	12.49
5.00	2.50	12.26
6.00	3.00	12.04
7.00	3.50	11.82
8.00	4.00	11.6
9.00	4.50	11.40
10.00	5.00	11.20

In Figure 2.5 (a-d) compares the Nusselt numbers given concerning (Seki et al., 1975) and calculated from the current study at each aspect ratio (AR =D_{out}/D_{in}) for both of the constant and variable Prandtl number approaches. Aspect ratio affects the variation of the Nusselt numbers as in the same way of the temperature changes. Nusselt number increases between the temperature difference range starting from 2°C to approximately 4-5°C. The temperature difference under discussion is between the inner and outer cases of the annulus. Beyond this peak point, the Nusselt number decreases as the temperature difference increases. The minimum Nusselt number is observed around the temperature difference of 6-7°C. Furthermore, increasing temperature difference yields the Nusselt number increase as well. Experimental results of the cited work (Seki et al., 1975) have a similar tendency with the current numerical findings. The current results are close to the experimental results of Seki et al. (1975), especially at cases having small annular spacing.

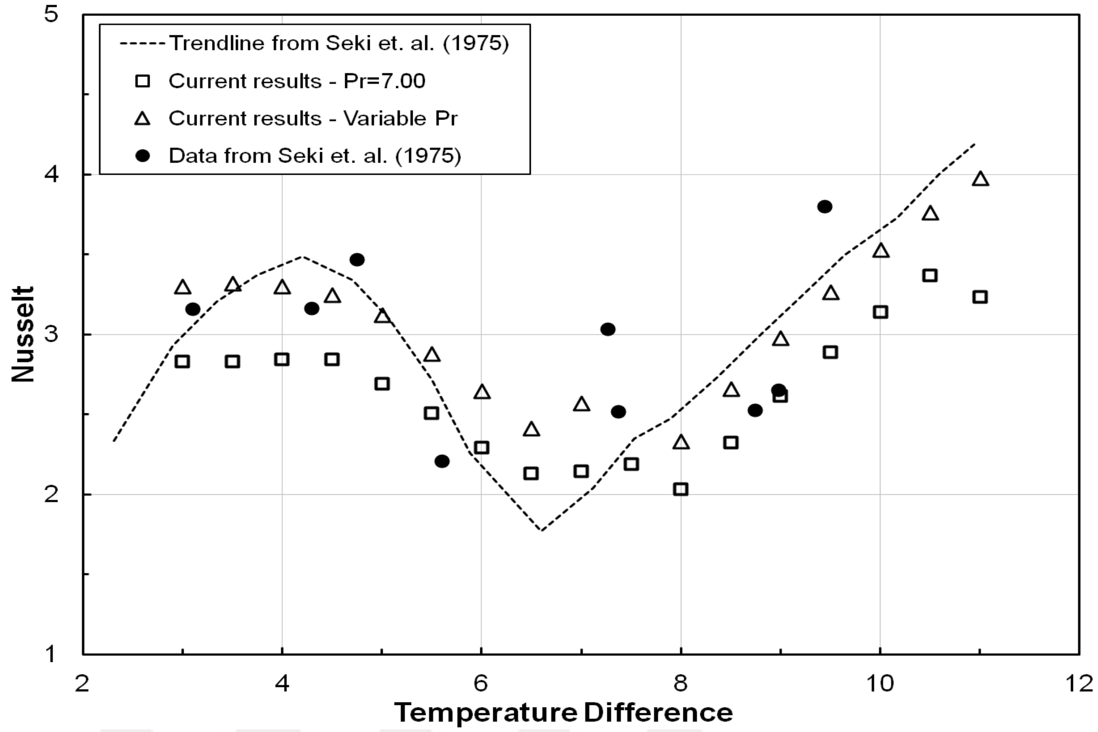

(a) AR = 1.72, T_{out} = 10°C

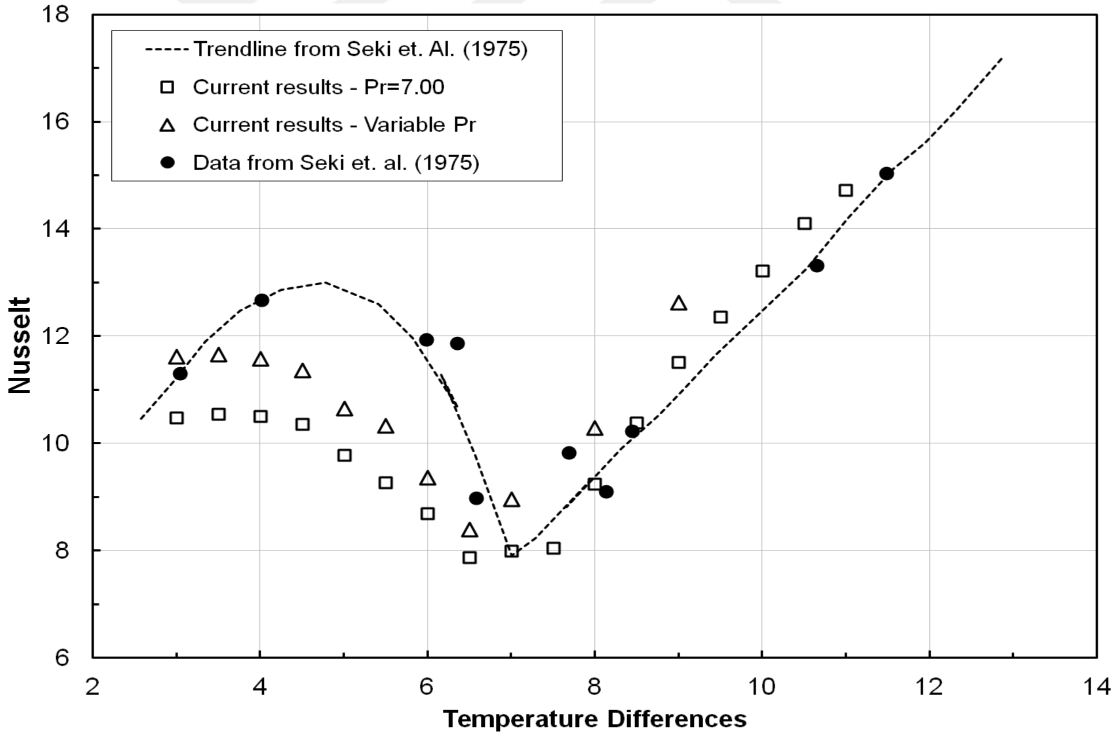

(b) AR = 3.20, T_{out} = 10°C

Figure 2.5 Variations of Nusselt number as a function of aspect ratio (AR) and temperature difference

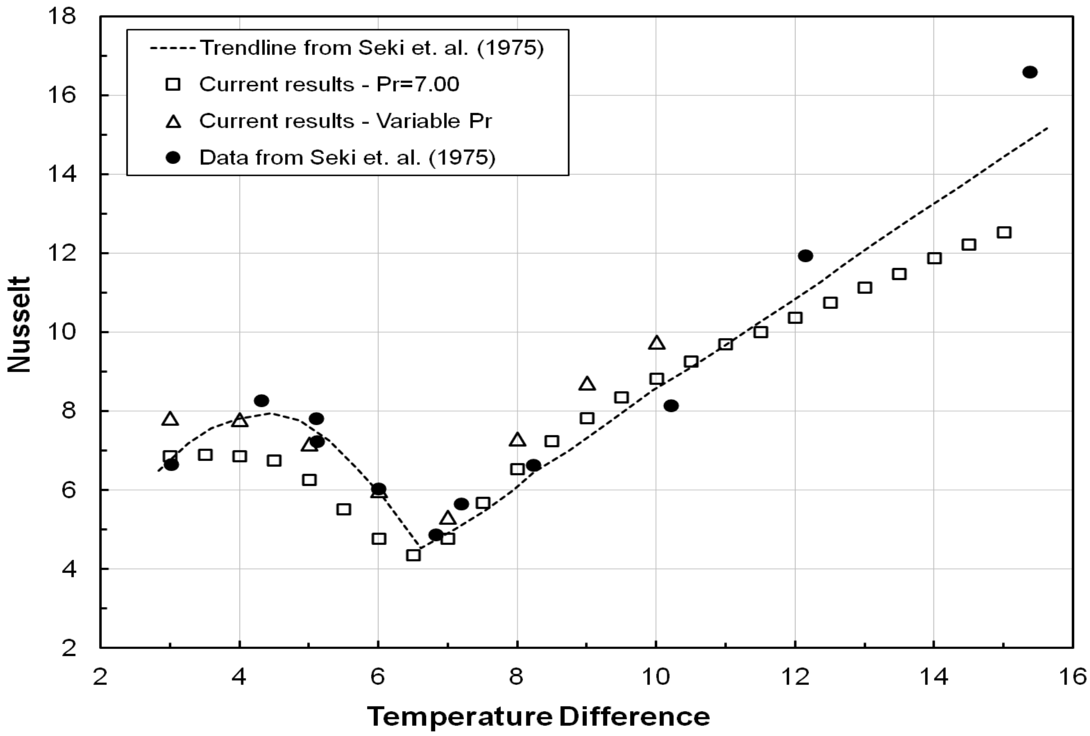

(c) AR = 3.44, T_{out} = 10°C

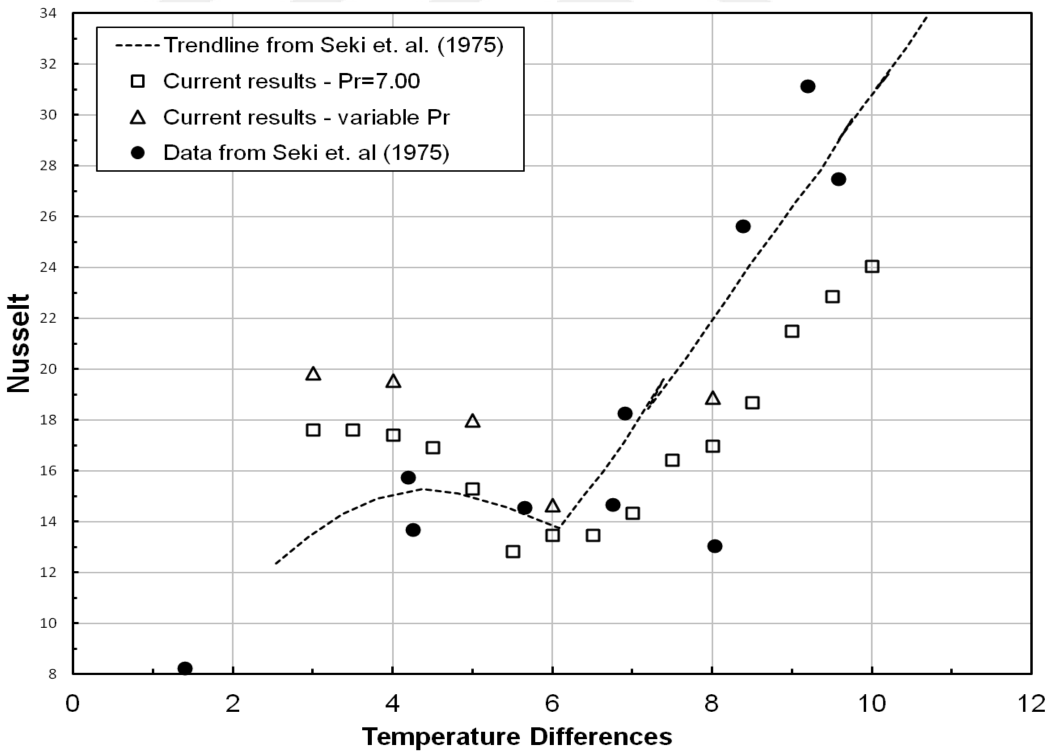

(d) AR = 6.39, T_{out} = 10°C

Figure 2.5 continues

2.4 Parametric Results for Water

After the verification with Seki et al. (1978), to investigate the density inversion effect, L/D_{in} and T_{in}-T_{out} (difference between inner and outer surface temperature) are changed from 0.4 to 1.0 and from 2°C to 12°C respectively. Nusselt number analyzed for hot inner surface and cold outer surface temperatures. It is clearly seen that the Nusselt number changes according to temperature differences. The Nusselt number first increases and then decreases and finally increases again. The reason for this tendency is viscous frictional forces between the circulation cells formed inside the annulus while the heat transfer occurs. This tendency is could be explained more clearly step by step. Three situations occur because of density changing. A circulation cell occurs at the first situation toward counterclockwise direction in a temperature range, which is from 2°C to 4°C. It is seen that the Nusselt number has a maximum value at 4°C. In the second situation, second circulation cell, which is the in the opposite direction to the other occurs, and Nusselt number starts to decrease, because of viscous frictions. At last situation, circulation cell has more significant effects on the other cell. So viscous frictions disappear. When the results of this study are observed, it is clear that the temperature at which Nusselt is minimum, natural convective velocity and the temperature difference between the walls are directly proportional to the ratio of L/D_{in} within the investigated range. When L/D_{in} increases, it is seen clearly that these values increase. L/D_{in} increases to 4°C, then decreases between 4°C and 9.5°C and finally, increases again. In other words, it can be said that the results of this study are compatible with previously published results.

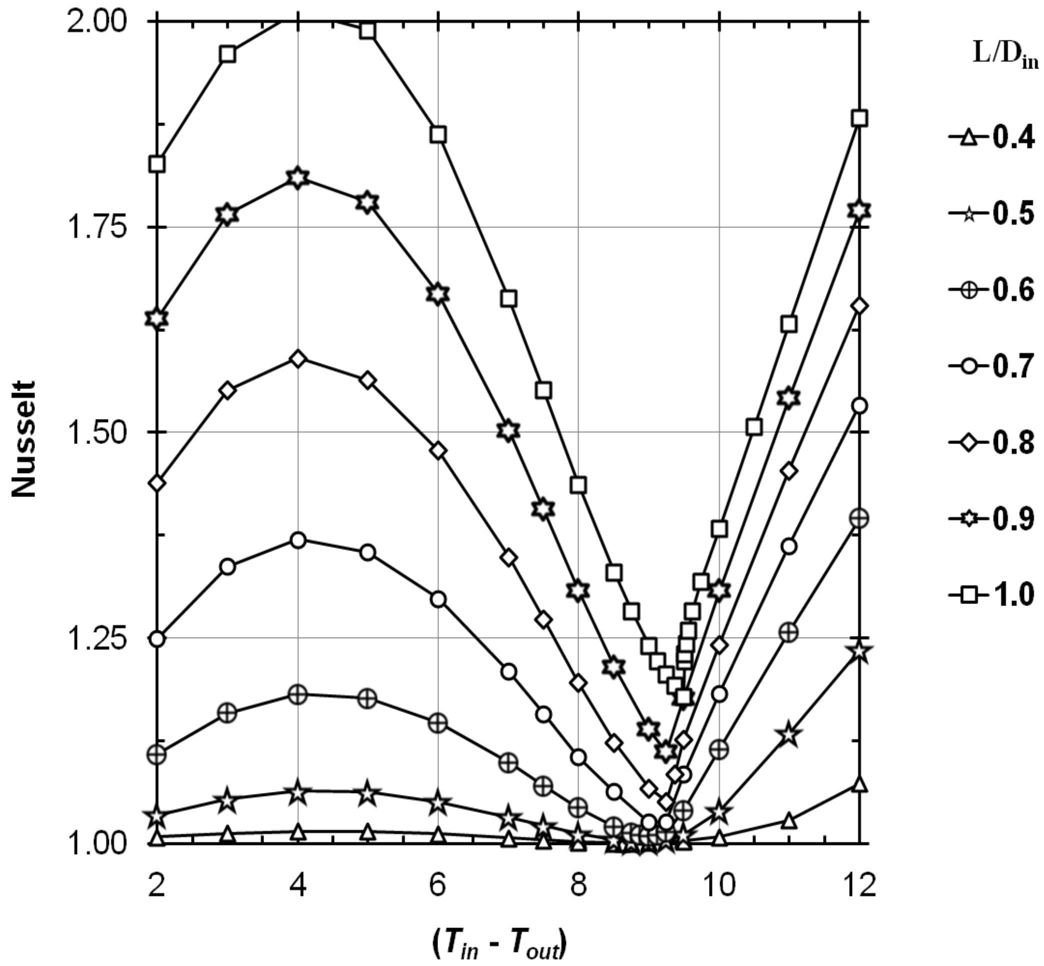

Figure 2.6 Variation of Nusselt number according to change of temperature difference at different L/D_{in} ratio

It could be noticed that the maximum Nusselt number is obtained at the temperature yielding maximum density. When the inner wall temperature exceeds 4°C, the Nusselt number decreases, and the minimum Nusselt number is obtained between 9.0°C and 9.5°C. Besides, in the case of the square cavity in cartesian coordinate, the minimum Nusselt number is obtained at 8°C (Kalfa & Ezan, 2016). In the cartesian geometry, the areas of the circulation cells are identical along the midline as the effect of buoyancy forces, and viscous frictions are symmetrical. However, for the cylindrical annulus, the surface area of the inner cylinder is smaller than the outer case, that is the buoyancy forces affecting the fluid are different along with the radial position.

In Figure 2.7, the temperature distributions and streamlines are given at three different inner temperatures of 4°C, 9°C, and 10°C. For the inner temperature of 4°C, the direction of the circulation cell is clockwise because water has maximum density value at 4°C and moves downward direction as seen from Figure 2.7 (a). The cold water adjacent to the outer cylinder has lower density and moves upward direction. In Figure 2.7(b) the flow pattern and temperature distributions are given for the outer temperature of 9°C. Even though a secondary circulation cell occurs, the isotherms resemble with the pure heat conduction case, due to low flow velocity. The viscous stress between opposite circulation cells reduces both the velocity of the fluid and rate of heat transfer from inner to the outer cylinder. When the inner wall temperature increases to 10°C, Figure 2.7(c), the direction of the dominant circulation cell is reversed. Warm water flows to the upper side of the annulus, as it has a lower density. Water cools down near the outer wall of the cylindrical annulus, and the density reduces. The cold water close to the outer wall flows to the opposite side of the main circulation cell.

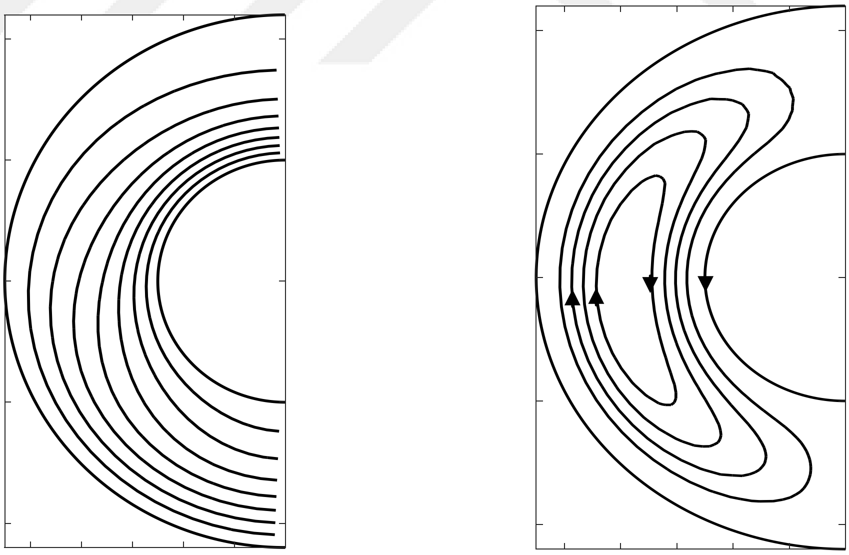

Temperature Distribution　　　　Streamlines

(a)

Figure 2.7 Temperature distribution and streamlines for different inner wall temperature (a) T_{in} = 4°C (b) T_{in} = 9°C (c) T_{in} = 10°C

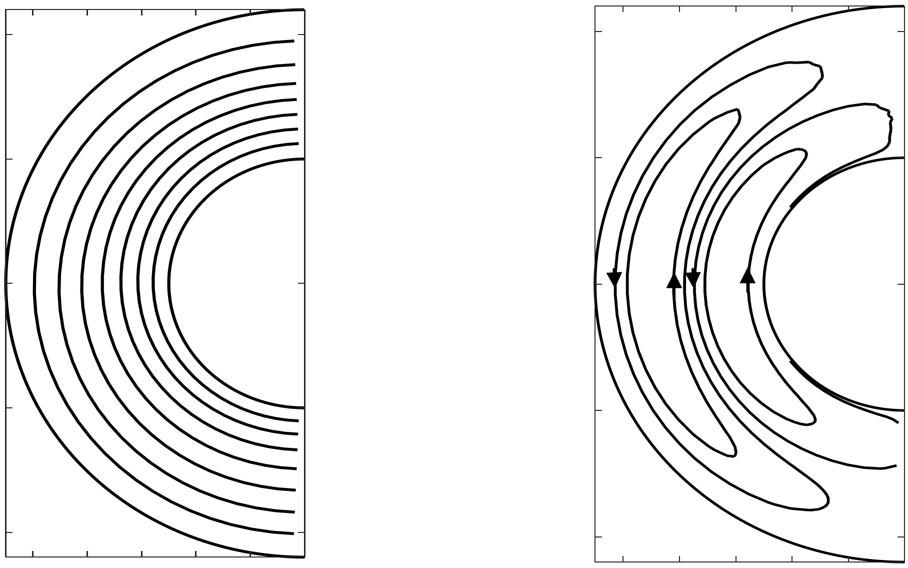

Temperature Distribution

Streamlines

(b)

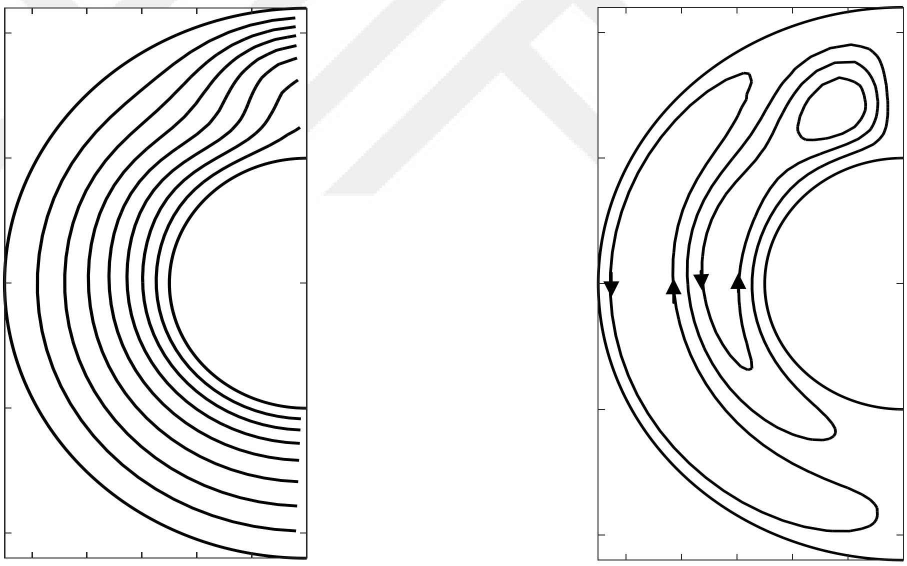

Temperature Distribution

Streamlines

(c)

Figure 2.7 continues

CHAPTER THREE

NATURAL CONVECTION DRIVEN PHASE CHANGE IN CYLINDRICAL ANNULUS

In this part of the thesis, natural convection-driven phase change phenomena in the cylindrical annulus are investigated. The melting of ice in the annulus is proposed to be analyzed by using MATLAB. The melting process is obtained for different values of the outer wall temperature of the cylinder, aspect ratio of the annulus and initial temperature of ice.

3.1 Definition of Problem

Natural convection-driven phase change inside the cylindrical annulus is investigated in a reduced 2D mathematical model by using MATLAB. The cylindrical annulus has inner and outer diameters are defined as D_{in} and D_{out}. Inner wall is adiabatic, and the outer wall temperature is kept at a uniform temperature of T_{out}. Water is initially at a uniform temperature of $T_{int,}$ which is lower than the melting point. In Figure 3.1, the geometry and boundary conditions are represented. The initial and boundary conditions are defined as below,

Initial condition:

$$t = 0 \qquad T(r,\theta) = T_{int}, \qquad u_r(r,\theta) = 0, \qquad u_\theta(r,\theta) = 0 \tag{3.1a}$$

r-direction:

$$r = R_{in} \qquad -k\frac{\partial T}{\partial r}\bigg|_{r=R_{in}} = 0, \qquad u_r = 0, \qquad u_\theta = 0 \tag{3.1a}$$

$$r = R_{out} \qquad T = T_{out}, \qquad u_r = 0, \qquad u_\theta = 0 \tag{3.1b}$$

θ-direction:

$$\theta = 0° \qquad -k\frac{\partial T}{\partial \theta}\bigg|_{\theta=0} = 0, \qquad \frac{\partial u_r}{\partial \theta}\bigg|_{\theta=0} = 0, \quad u_\theta = 0 \tag{3.1c}$$

$$\theta = 180° \qquad -k\frac{\partial T}{\partial \theta}\bigg|_{\theta=\pi} = 0, \qquad \frac{\partial u_r}{\partial \theta}\bigg|_{\theta=\pi} = 0, \; u_\theta = 0 \tag{3.1d}$$

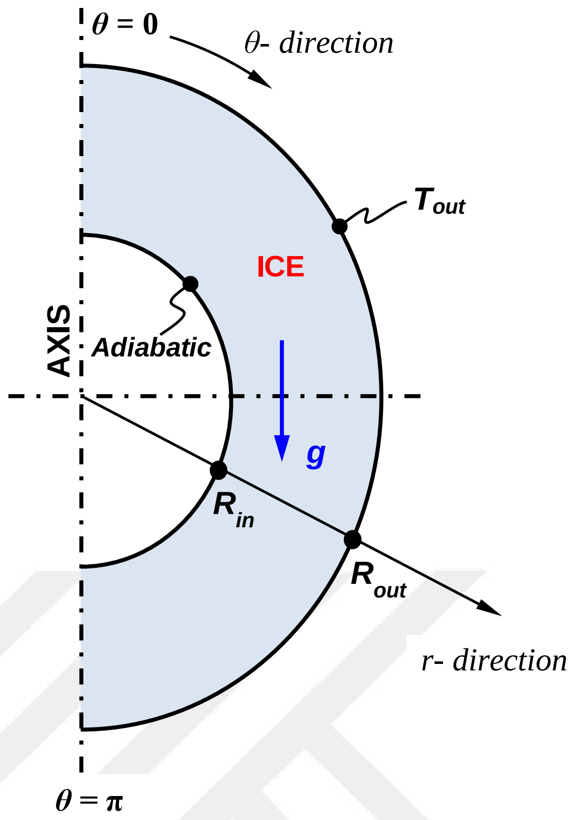

Figure 3.1 Schematic view of the 2D annulus with the defined boundary conditions

3.2 Solution Method

Following reductions are considered to simplify the inward melting of ice,

- Two-dimensional and axis-symmetric geometry,
- PCM is incompressible, and the type of flow is laminar.

For the cylindrical coordinates system, *mass* and *r*- and θ-momentum equations are the same with equations in 2.2, 2.3, and 2.4. Besides, the energy equation is modified from the enthalpy form to consider the internal energy variation due to the phase change. The energy equation is defined in terms of the enthalpy as below,

$$\frac{\partial H}{\partial t} + u_r \frac{\partial H}{\partial r} + \frac{u_\theta}{r}\frac{\partial H}{\partial \theta} = k\left[\frac{1}{r}\frac{\partial}{\partial r}\left(r\frac{\partial T}{\partial r}\right) + \frac{1}{r^2}\frac{\partial}{\partial \theta}\left(\frac{\partial T}{\partial \theta}\right)\right] \tag{3.2}$$

Temperature transformation method is applied to define the energy equation in terms of the temperature, rather than the enthalpy form (Dinçer & Ezan, 2018) Enthalpy of a matter is formulated as a summation of the sensible and latent heat components in Equation 3.3,

$$H = h + \rho h_{sf} f \tag{3.3}$$

Here, h is sensible enthalpy, f is the liquid fraction of the material, and h_{sf} is latent heat. The sensible enthalpy of the matter could be written as

$$\frac{dh}{dT} = \rho c \tag{3.4}$$

Integration of this equation yields,

$$h = h_{ref} + \int_{T_{ref}}^{T} (\rho c) dT \tag{3.5}$$

In the temperature transforming method, it is assumed that there is a linear variation between temperature and enthalpy. Moreover, three different phases, which are solid, mushy, and liquid, are considered to simplify the numerical solution of the phase change (Figure 3.2). The enthalpy each phase can be written as below (Dinçer & Ezan, 2018),

$$H(T) = \begin{cases} C_s(T - T_m) + C_s \delta T_m & for\ solid\ phase \\ \left(C_m + \rho \dfrac{h_{sf}}{2\delta T_m}\right)(T - T_m + \delta T_m) & for\ mushy\ phase \\ C_l(T - T_m) + C_s \delta T_m + \rho h_{sf} & for\ liquid\ phase \end{cases} \tag{3.6}$$

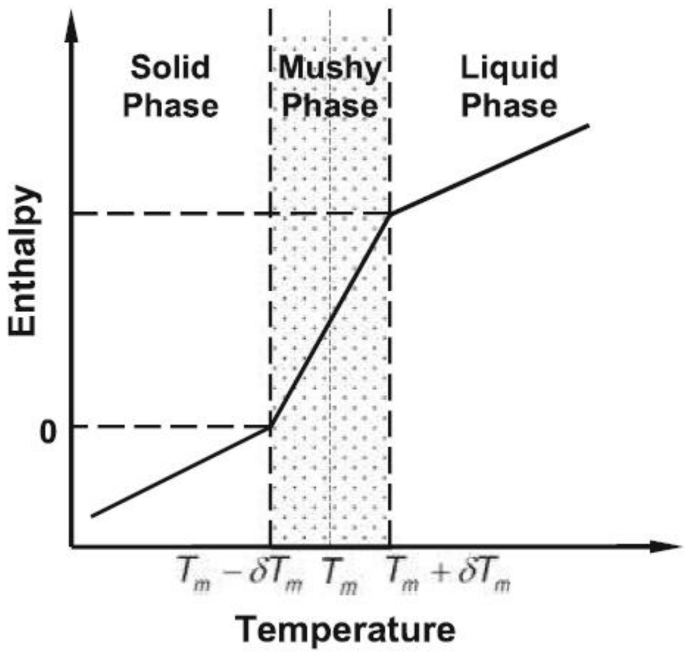

Figure 3.2 Relationship between Enthalpy-Temperature for three phases (Dinçer & Ezan, 2018)

Following linear function is assumed to express the relationship between the enthalpy and the temperature,

$$H = CT + S \tag{3.7}$$

where C is the volumetric heat capacity, and S is source term. For each phase, C and S terms are evaluated as

$$C(T) = \begin{cases} C_s & for\ solid\ phase \\ C_m + \rho \dfrac{h_{sf}}{2\delta T_m} & for\ mushy\ phase \\ C_l & for\ liquid\ phase \end{cases} \tag{3.8}$$

$$S(T) = \begin{cases} C_s \delta (T - T_m) & for\ solid\ phase \\ \left(C_m + \rho \dfrac{h_{sf}}{2\delta T_m} \right) (\delta T_m - T_m) & for\ mushy\ phase \\ C_s \delta T_m - C_l T_m + \rho h_{sf} & for\ liquid\ phase \end{cases} \tag{3.9}$$

Implementation of the temperature transforming method yields the following energy equation for cylindrical coordinates in temperature-based form,

$$
\begin{aligned}
&\frac{\partial(CT)}{\partial t}+u_r\frac{\partial(CT)}{\partial r}+\frac{u_\theta}{r}\frac{\partial(CT)}{\partial\theta}\\
&=k\left[\frac{1}{r}\frac{\partial}{\partial r}\left(r\frac{\partial T}{\partial r}\right)+\frac{1}{r^2}\frac{\partial}{\partial\theta}\left(\frac{\partial T}{\partial\theta}\right)\right]-\frac{\partial S}{\partial t}-u_r\frac{\partial S}{\partial r}\\
&-\frac{u_\theta}{r}\frac{\partial S}{\partial\theta}
\end{aligned}
\tag{3.10}
$$

where S is constant in the liquid phase, and velocity components are zero in the solid phase. Thus, the two terms on the right-hand side of Equation (3.10), which contain u_r and u_θ velocity components are omitted. Rearranging Equation (3.11) yields the following final form of the energy equation for the phase change problem,

$$
\begin{aligned}
&\frac{\partial(CT)}{\partial t}+u_r\frac{\partial(CT)}{\partial r}+\frac{u_\theta}{r}\frac{\partial(CT)}{\partial\theta}\\
&=k\left[\frac{1}{r}\frac{\partial}{\partial r}\left(r\frac{\partial T}{\partial r}\right)+\frac{1}{r^2}\frac{\partial}{\partial\theta}\left(\frac{\partial T}{\partial\theta}\right)\right]-\frac{\partial S}{\partial t}
\end{aligned}
\tag{3.11}
$$

The solution methods that are described in Chapter 2 are implemented here to resolve the governing equations iteratively.

3.3 Validation

First of all, the developed model is validated numerically to compare the results with reference to White et al., (1986). When Ra number is large enough, natural convection circulation starts. The ice starts to melt at the inner surface of the annulus. At T_w < 8°C, liquid water starts to circulate below the cylinder, and liquid region increases. In this situation, the shape of the solid/liquid interface resembles an upside-down pear. When T_w >8°C, the liquid region occurs above the cylinder. Recirculation starts here, and in this situation, the shape of the liquid water region is as an up-right pear.

A dimensionless liquid volume is defined as follows (White et al., 1986) to evaluate the variation of the interface growth,

$$V^* = \frac{V - V_0}{V_0} \tag{3.12}$$

In this formulation, V is the volume of liquid water, and V_o is the volume of the cylinder. Dimensionless liquid volume is related to interface position, i.e., r, and Rayleigh number. In Figure 3.3, dimensionless liquid volume ratio is compared with data, which is given in the reference paper. Compression is done for different wall temperature of the cylinder. As a result, when the surface temperature of the cylinder increases, it is observed that the proportion of dimensionless liquid water is formed in a shorter time. Obtained results are compatible with the data regarding White, Bathelt, Leidenfrost & Viskanta (1977).

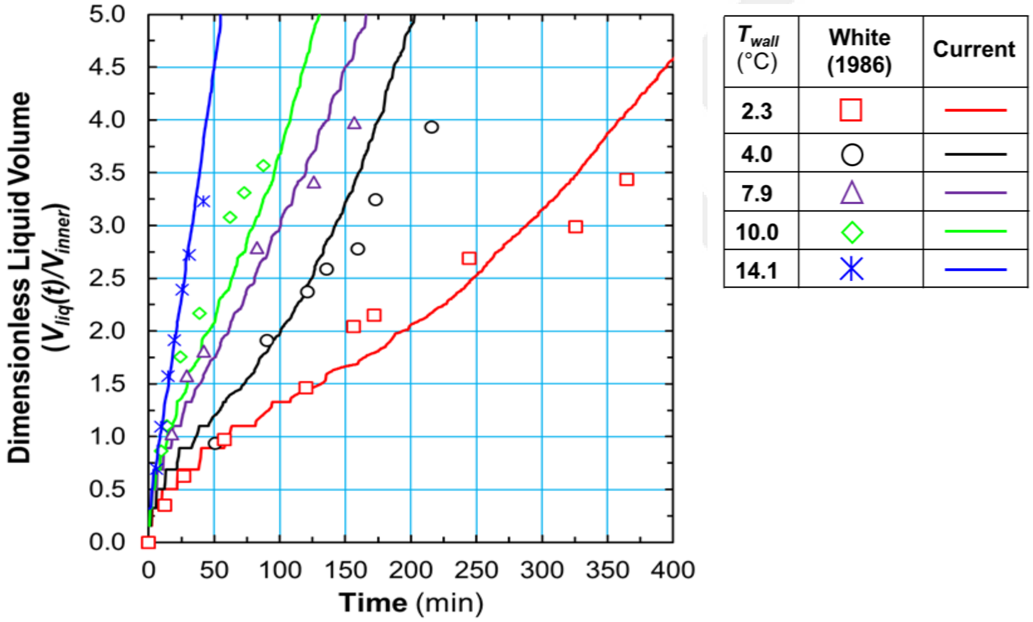

Figure 3.3 Variation of dimensionless liquid volume respect by the time

3.4 Parametric Analyses

Parametric simulations are performed at three different temperature, 4°C, 8°C, and 14°C, respectively. For each temperature, beginning of the melting, conduction is the dominant heat transfer mechanism as against convection. During this time, the solid-liquid phase has circle shape, and its center coincident with the axis of the cylindrical annulus. While melting continues, convection which is in the melting area intensifies and for this reason isotherms become deformed.

When the inner wall temperature, T_w is at 4°C, the water close to the inner cylinder has the highest density. So, flow gravitates below the cylindrical annulus, as in Figure 3.4. Water locates between the inner cylinder wall and ice.

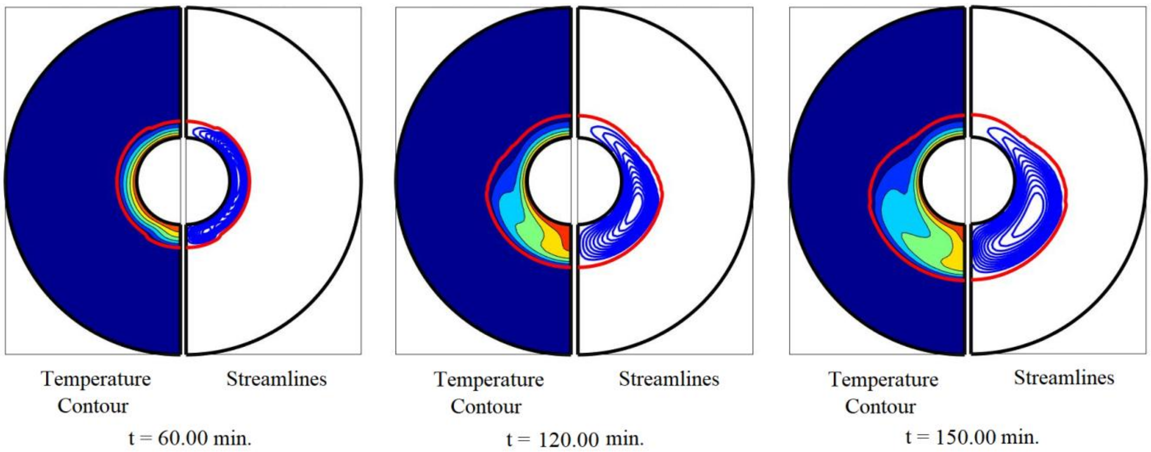

Figure 3.4 The temperature field (right) and the flow field (left) for T_w = 4°C

At T_w is 8°C, the temperature distributions and flow fields are obtained. They are given in Figure 3.5 for different time steps. Meanwhile, two discrete vortexes which circulate opposite directions appear in the melting region. While the melting continuous, outer vortex next to the ice intensifies. As a result of this period, outer vortex sprawls. It is observed that the melting area is more extensive at the underside of the cylindrical annulus.

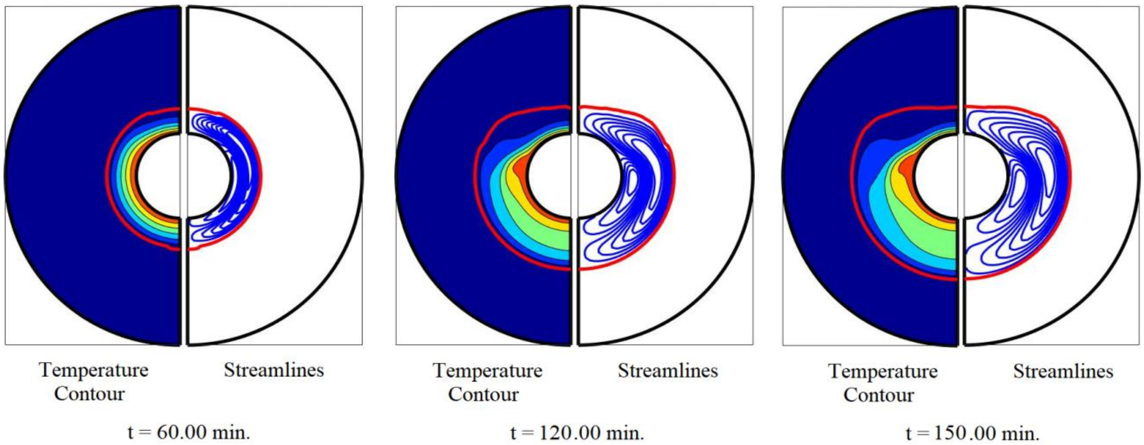

Figure 3.5 The temperature field (right) and the flow field (left) for T_w = 8°C

Figure 3.6 shows the results for T_w>14°C. At the beginning of the melting, the pear shape is formed above the inner cylinder. Melting is more at this side of the cylindrical annulus. The second vortex locates below the annulus. Bigger vortex continues to get large above the annulus during this period. Meanwhile, the liquid water region reaches the outer cylinder.

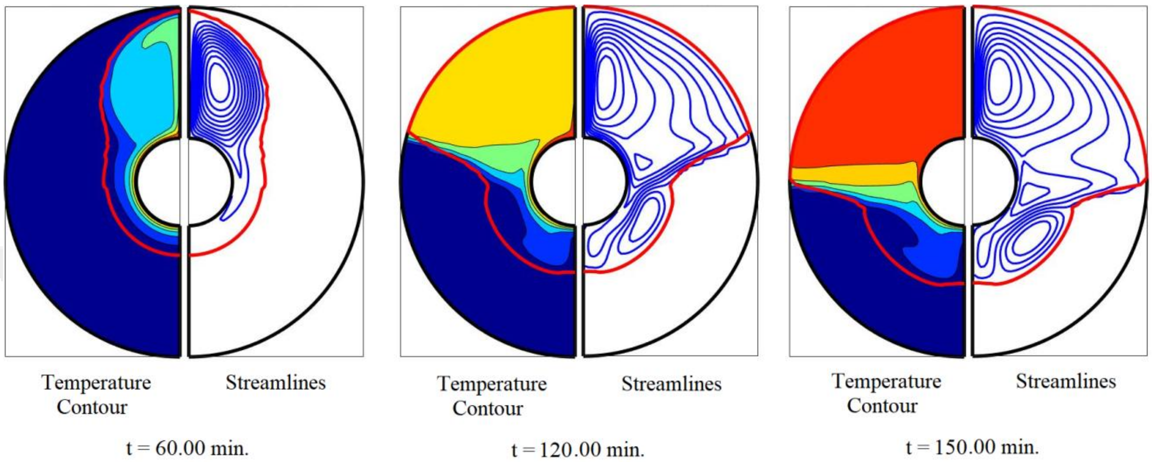

Figure 3.6 The temperature field (right) and the flow field (left) for T_w = 14°C

Liquid volume ratio is the fraction of the liquid water region volume and heat source volume. Time depended behavior of the liquid water volume ratio is shown in Figure 3.6. It is obviously seen that the results of this study are compatible with the results of the literature (White et al., 1986).

Diagrams in Figure 3.7 (a-c) show that the melting time with various temperatures for three different aspect ratios (AR). When the temperature increases, it is clearly seen that melting time decreases step by step for each AR ratio. If Figure 3.7 (a) is considered, when temperature is at 2°C, melting process finishes at 352 minutes. This is the maximum melting time. On the other hand, melting time gradually decreases to 142, 74 and 42 minutes, when temperature differences are at 4, 8 and 12°C respectively. This decreasing of melting time occurs for other aspect ratios at different temperature differences.

From another perspective, when AR increases, the melting time of ice is quitely increasing. If the melting time of a single temperature differences at different aspect ratios is considered, such as 12°C, it is seen that melting time increases as long as aspect ratio increases. When the aspect ratio is 2, melting time is 42 minutes. However, melting time increases to 110 and 192 minutes, when the aspect ratio is 4 and 8, respectively. In Figure 3.8 (a-d) shows the temperature contours and streamlines at AR=4 and AR=8 with different temperatures and time steps. These mentioned variations are clearly seen from these illustrations.

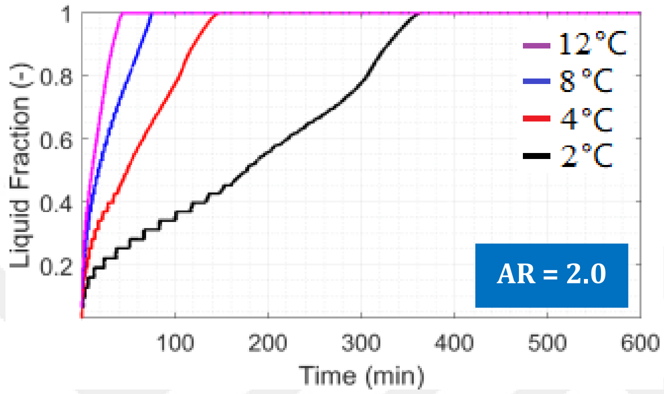

2°C	357 min
4°C	142 min
8°C	74 min
12°C	42 min

(a)

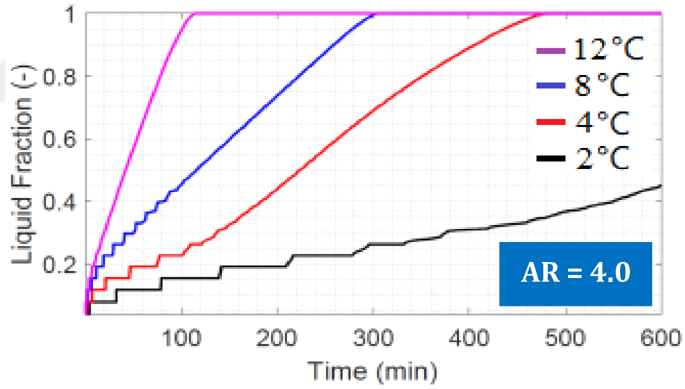

2°C	0.44
4°C	467 min
8°C	297 min
12°C	110 min

(b)

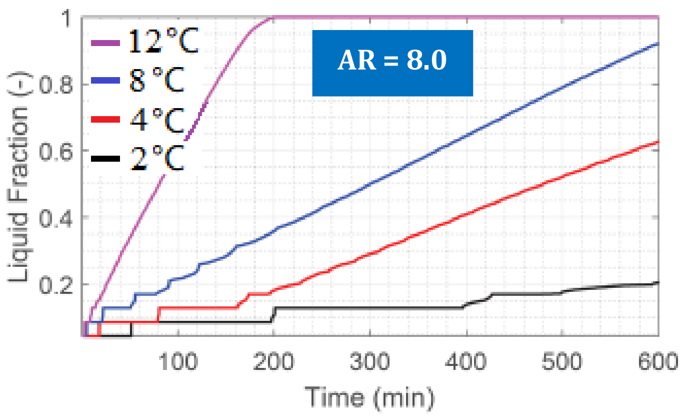

2°C	0.20
4°C	0.63
8°C	0.92
12°C	192 min

(c)

Figure 3.7 Variation of liquid fraction respect by time with different AR ratio

The most prominent variations of the temperature contours and streamlines are obtained at 500. minutes, in Fıgure 3.8 (a). Because temperature differences are quitely low and melting is occurs slowly in this condition. Although in Figure 3.8 (b) has the same AR with (a), when temperature differences are increased, variations of the temperature contours and streamlines can be more obviously monitored.

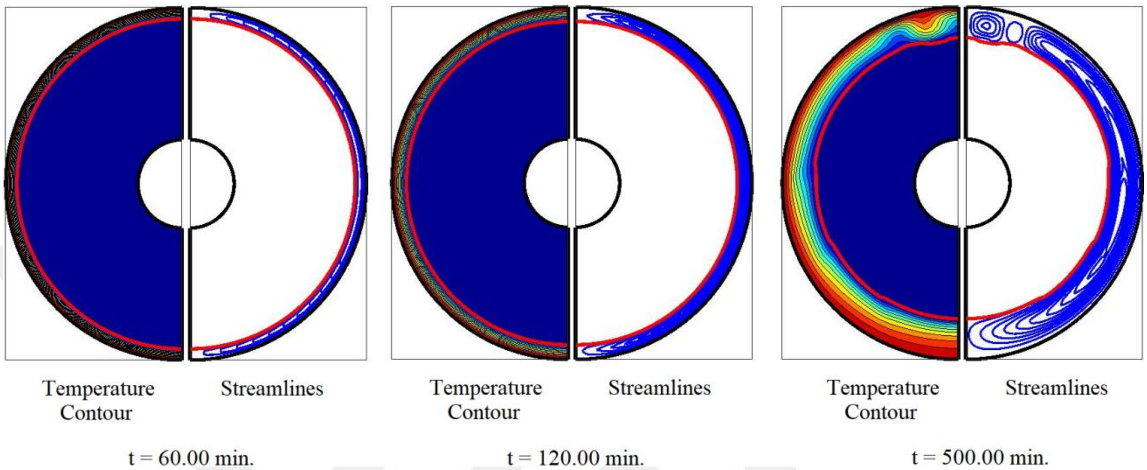

(a) AR = 4 and ΔT = 2°C

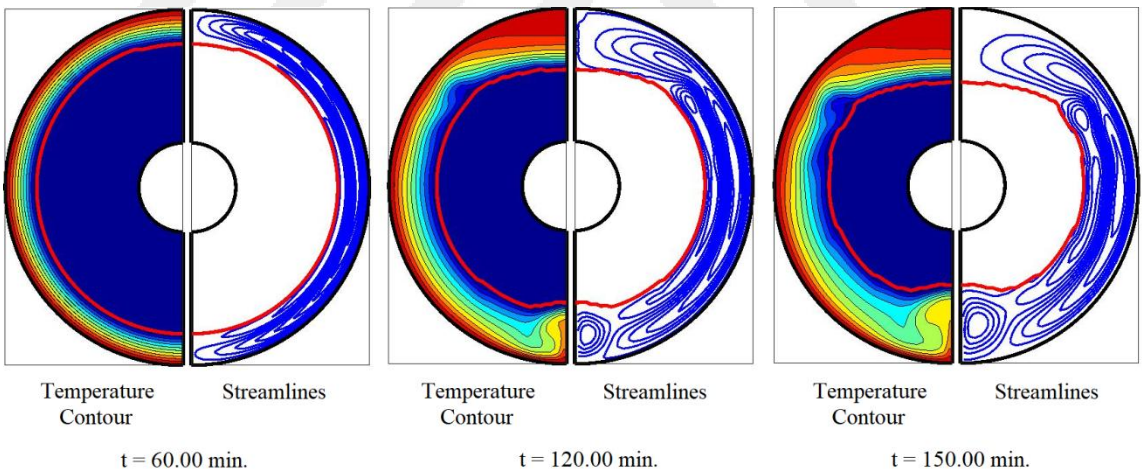

(b) AR = 4 and ΔT = 8°C

Figure 3.8 Temperature contours and streamlines at different AR and ΔT at different times

In the same way, when the aspect ration is 8, if temperature difference is low, the melting occurs slowly. However, melting is fast, when temperature differences increases although effects of increasing the aspect ratio on melting is negatively.

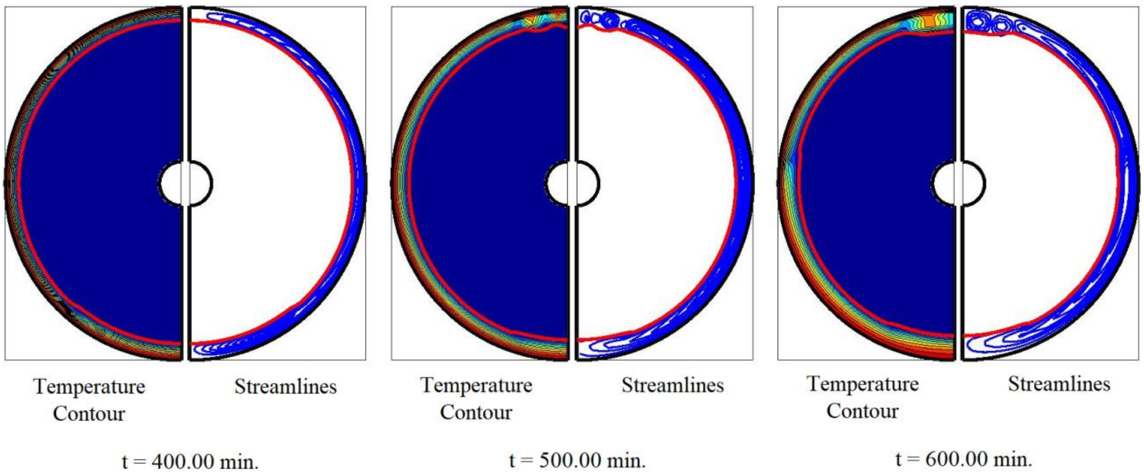

(c) AR = 8 and ΔT = 2°C

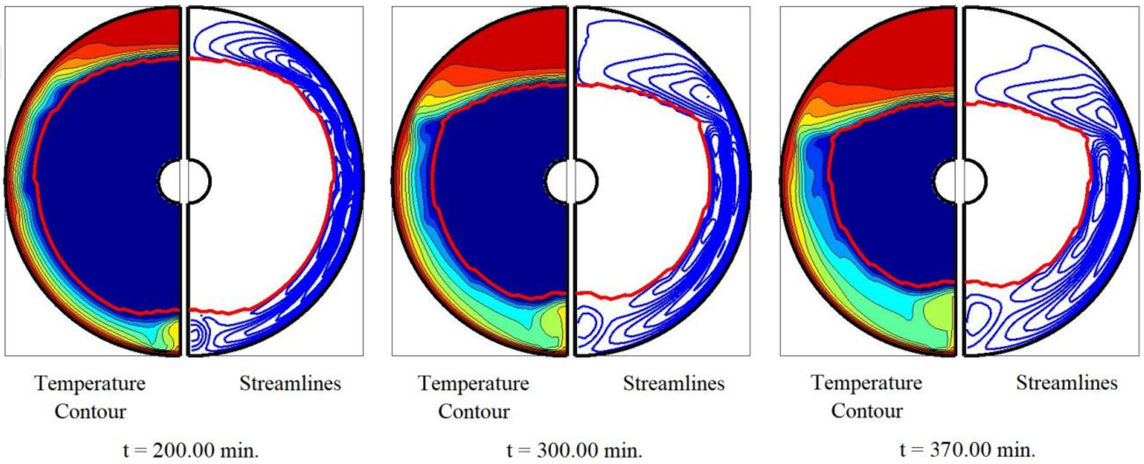

(d) AR = 8 and ΔT = 8°C

Figure 3.8 continues

CHAPTER FOUR
CONCLUSION

In the current thesis, three different problems are studied and compared with other studies in the literature. CFD code is developed in MATLAB to be solved this problem.

In the first case, created model is performed for air (Pr=0.7). Variation of the Nusselt number depending on Rayleigh number is observed and compared with findings in the literature. In other respects, variation of the Nusselt number are obtained for both cylinder, according to angular position. Nusselt number increases from 0° to 180° at inner cylinder by contrast with outer cylinder. The results are found to be compatible with the literature. Thus, the code is validated.

Secondly, code is performed again to investigate the natural convection for water domain. At first case, when Prandlt number is constant (Pr=7), The temperature of the inner cylinder is increased step by step. At the second case for water that Prandlt number is depended of the temperature function. Occurred viscous friction forceses are watched between the vortexes. Variation of the Nusselt number is observed depending on occurred forceses. The results are matched with literature findings. All the results are compatible with the literture findings.

Finally, phase change of ice within the cylindrical annulus is examined. Analyses are done for three different temperatures and three different aspect ratios. The temperature difference and the duration of the phase change are inversely proportional. Besides, the aspect ratio and the duration of the phase change are directly proportional. At the same time, occurred liquid water during the phase change is examined. The results are compared with literature. All the results are appropriate with the literature.

REFERENCES

Abdulateef, A. M., Mat, S., Sopian, K., Abdulateef, J., & Gitan, A. A. (2017). Experimental and computational study of melting phase-change material in a triplex tube heat exchanger with longitudinal/triangular fin. *Solar Energy, 155,* 142-153.

Abdulateef, A. M., Mat, S., Abdulateef, J., Sopian, K. & Al-Abidi, A. A. (2018). Thermal Performance Enhancement of Triplex Tube Latent Thermal Storage Using Fins-Nano- Phase Change Material Technique. *Heat Transfer Engineering*, *39*(12), 1067-1080.

Agyenim, F., Hewitt, N., Eames, P. & Smyth, M. (2010). A review of materials, heat transfer and phase change problem formulation for latent heat thermal energy storage systems (LHTESS). *Renewable and Sustainabşe Energy Rewievs, 14*(2), 615-628.

Bergman, L., Lavine, A.S., Incropera, F.P., & De Witt, D.P. (2011). *Fundamentals of heat and mass transfer*. New York: John Wiley & Sons.

Bhutta, M. M. A., Hayat, N., Bashir, M. H., Khan, A. R., Ahmad, K. N., & Khan, S. (2012). CFD applications in various heat exchangers design: A review. *Applied Thermal Energy, 32,* 1-12.

Darzi, A. A. R., Jourabian, M., & Farhadi, M. (2016). Melting and solidification of PCM enhanced by radial conductive fins and nanoparticles in cylindrical annulus. *Energy Conversion and Management, 118*(15), 253-263.

Deng, S., Nie, C., Wei, G., & Ye, W. (2019). Improving the melting performance of a horizontal shell-tube latent-heat thermal energy storage unit using local enhanced finned tube. *Energy and Building, 183*(15), 161-173.

Dinçer I. & Ezan M. A. (2018). *Heat storage: A unique solution for energy storage* Berlin: Springer.

Dolado, P., Lazaro, A., Marin, J. & M., Zalba, B. (2011). Characterization of melting and solidification in a real scale PCM-air heat exchanger: Numerical model and experimental validation. *Energy Conversion and Mangement, 52*(4), 1890-1907.

Gençer, A. E., Ezan, M. A., Yavuz, F. E., Alptekin, E., & Erek, A. (2017). Numerical modelling of natural convectıve heat transfer in cylindrical annulus. *ULIBTK'17 21. Ulusal Isı Bilimi ve Tekniği Kongresi Bildiri Kitabı,* 894-900.

Ezan, M. A., & Kalfa, M. (2016). Numerical investigation of transient natural convection heat transfer of freezing water in a square cavity. *International Journal of Heta and Fluid Flow, 61*(B), 438-448.

Kuehn T. H., & Goldstein, R. J. (1976). An experimental and theoretical study of natural convection in the annulus between horizontal concentric cylinders. *Journal of Fluid Mechanics, 74*(4), 695-719.

Liu, Z., Sun, X. & Ma, C. (2005). Experimental investigations on the characteristics of melting processes of stearic acid in an annulus and its thermal conductivity enhancement by fins. *Energy Conversion and Management, 46*(6), 959-969.

Mao, Q. (2016). Recent developments in geometrical configurations of thermal energy storage for concentrating solar power plant. *Renewable and Sustainable Energy Reviews, 59,* 320-327.

Mat, S., Al-Abidi, A. A., Sopian, K., Sulaiman, M. Y., & Th Mohammada, A. (2013). Enhance heat transfer for PCM melting in triplex tube with internal–external fins. *Energy Conservion and Management, 74,* 223-236.

Medrano, M., Yilmaz, M.O., Nogués, M., Martorell, I., Roca, J., & Cabeza, L. F. (2009). Experimental evaluation of commercial heat exchangers for use as PCM thermal storage systems. *Applied Energy, 86*(10), 2047-2055.

Parry, A. J., Eames. P. C., & Agyenim, F. B. (2014). Modeling of Thermal Energy Storage Shell-and-Tube Heat Exchanger. *Heat Transfer Engineering, 35*(1), 1-14.

Patankar, S. V., (1980), *Numerical heat and fluid flow*. New York: Hemisphere.

Pizzolato, A., Sharma, A., Maute, K., Sciacovellic, A., & Verda, V. (2017). Design of effective fins for fast PCM melting and solidification in shell-andtube latent heat thermal energy storage through topology optimization. *Applied Energy, 208*(15), 210-227.

Rahnama, M., & Farhadi, M. (2004). Effect of radial fins on two-dimensional turbulent natural convection in a horizontal annulus. *Internation Journal of Thermal Sciences, 43*(3), 255-264.

Seki, N., Fukusako, S., & Nakaoka, M. (1975). Exiperimental Study on Natural Confection Heat Transfer With Density Inwersion of Water Between Two Horizontal Concentric Cylinders. *Journal of Heat Transfer, 97*(4), 556-561.

Seki, N., Fukusako, S., & Inaba H. (1978). Free convective heat transfer with density inversion in a confined rectangular vessel. *Warme-und Stoffübertragung, 11*(3), 145-156.

Shu, C., Yao, Q., Yeo, K. S., & Zhu, Y. D. (2002). Numerical analysis of flow and thermal fields in arbitrary eccentricannulus by differential quadrature method. *Heat and Mass Transfer, 38*(7-8), 597-608.

Tiari, S., Qiu, S., & Mahdavi, M. (2015). Numerical study of finned heat pipe-assisted thermal energy storage system with high temperature phase change material. *Energy Conversion and Management, 89*(1), 833-842.

White, R. D., Bathelt, A. G., Leidenfrost, W. & Viskanta, R. (1977). *Study of heat transfer and melting from a cylinder imbedded in a phase change material.* ASME Paper No. 77-HT-42, American Society of Mechanical Engineers, New York.

White, R. D., Viskanta, R., & Leidenfrost, W. (1986). Heat transfer during the melting of ice around a horizontal, isothermal cylinder. *Experiment in Fluids, 4*(3), 171-179.

Yavuz, F. E. (2017). *Natural convection driven phase change inside spherical capsule.* MSc Thesis, Dokuz Eylul University, İzmir.

APPENDICES

Nomenclature

c	Specific heat (J/kgK)
C	Volumetric heat capacity (J/Km^3)
D	Diameter of cylinder (m)
f	Liquid fraction
h	Specific enthalpy (J/m^3)
H	Volumetric enthalpy (J/m^3)
k	Thermal conductivity (W/mK)
L	Difference between inner and outer radii (m)
Nu	Nusselt number
Pr	Prandtl number
q	Rate of heat transfer (W)
Ra	Rayleigh number
R	Radii of cylinder (m)
S	Source term (J/m^3)
T	Temperature (K or C)
u,v	Velocity components (m/s)
V	Volume of liquid water (m^3)
$v*$	Dimensionless liquid volume
V_o	Volume of the cylinder (m^3)

Subscripts and Superscripts

m	Mushy zone
s	Solid
in	Inner
out	Outer
r	Radial

θ	Polar cordinate
Δ	Difference
ref	Reference
sf	Solid to fluid
c	Cold
h	Hot
w	Wall

Greek Letters

α	Thermal Diffusivity (m^2/s)
β	Thermal expansion coefficient (1/K)
δ	Width of the PCM channel (m)
ϑ	Kinematic Vicosity (m^2/s)
ρ	Density (kg/m^3)

Abbreviations

AR	Aspect ratio
CFD	Computational Fluid Dynamics
HTF	Heat Transfer Fluid
LHTES	Latent Heat Transfer Fluid
LPM	Lumped Parameters Modelling
PCM	Phase Change Material
SIMPLE	Semi Implicit Method for Pressure Linked Equations
TES	Thermal Energy Storage
TTHX	Triplex Tube Heat Exchanger